Conformal Prediction for Semantically-Aware Autonomous Perception in Urban Environments

Achref Doula Tobias Güdelhöfer Max Mühlhäuser Alejandro Sanchez Guinea
Telecooperation Lab
Technical University of Darmstadt, Germany
{doula, max, sanchez}@tk.tu-darmstadt.de

Abstract:
We introduce Knowledge-Refined Prediction Sets (KRPS), a novel approach that performs semantically-aware uncertainty quantification for multitask-based autonomous perception in urban environments. KRPS extends conformal prediction (CP) to ensure 2 properties not typically addressed by CP frameworks: semantic label consistency and true label coverage, across multiple perception tasks. We elucidate the capability of KRPS through high-level classification tasks crucial for semantically-aware autonomous perception in urban environments, including agent classification, agent location classification, and agent action classification. In a theoretical analysis, we introduce the concept of semantic label consistency among tasks and prove the semantic consistency and marginal coverage properties of the produced sets by KRPS. The results of our evaluation on the ROAD dataset and the Waymo/ROAD++ dataset show that KRPS outperforms state-of-the-art CP methods in reducing uncertainty by up to 80% and increasing the semantic consistency by up to 30%, while maintaining the coverage guarantees.

Keywords: Robot Perception, Uncertainty in Robotics, Semantics for Robotics

1 Introduction

In urban environments, autonomous systems are tasked with navigating complex and dynamic scenes, necessitating robust decision-making mechanisms that can interpret diverse elements with a high-level semantic understanding. To reason about the scene, autonomous systems perform a series of critical tasks, distinguishing between different types of agents like pedestrians and vehicles, understanding their actions such as walking, turning, or stopping, and identifying their locations relative to key infrastructure like crosswalks and intersections [1, 2, 3, 4, 5, 6]. Such tasks require the construction of semantic relationships between scene elements to ensure safety and enhance model interpretability [7, 8, 9]. However, the inherent unpredictability of urban environments and the safety-critical applications of autonomous perception in urban environments make it essential to integrate semantically-aware reasoning with uncertainty quantification. Combining semantic and uncertainty awareness allows autonomous agents to make reliable and contextually appropriate decisions, adapting to the urban landscape dynamically.

Conformal prediction (CP) [10, 11, 12] emerges as a versatile approach for uncertainty quantification in learning-based models. Compared to other uncertainty quantification frameworks in deep learning, such as Bayesian networks [13], Radial Basis Functions networks [14], and evidential learning [15], CP provides uncertainty-aware predictions by generating prediction sets that are theoretically guaranteed to include the correct class with user-defined confidence. The guarantees offered by CP-based frameworks ensure the reliability of the underlying systems, a property that is much needed to improve trust and large-scale adoption of autonomous systems interacting with urban environments. CP has been effectively applied in various areas of robotics, including robot manipu-

8th Conference on Robot Learning (CoRL 2024), Munich, Germany.

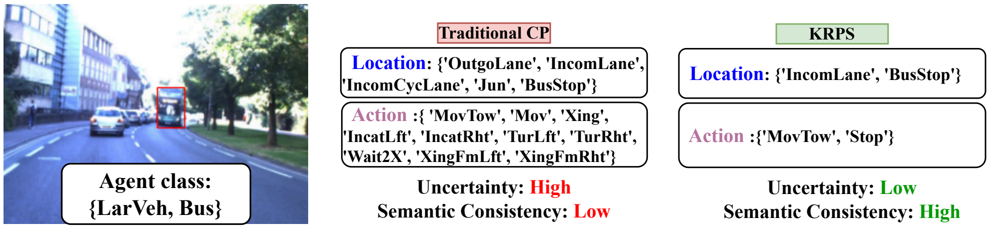
Agent class:
{LarVeh, Bus}
Traditional CP
Location: {'OutgoLane', 'IncomLane', 'IncomCycLane', 'Jun', 'BusStop'}
Action :{ 'MovTow', 'Mov', 'Xing', 'IncatLft', 'IncatRht', 'TurLft', 'TurRht', 'Wait2X', 'XingFmLft', 'XingFmRht'}
Uncertainty: High
Semantic Consistency: Low
KRPS
Location: {'IncomLane', 'BusStop'}
Action :{'MovTow', 'Stop'}
Uncertainty: Low
Semantic Consistency: High

(a) Situation (b) Traditional CP (c) KRPS

Figure 1: An example of refined sets using KRPS on a scene from the ROAD dataset [1]. KRPS reduces the location set size by 60% and the action set size by 80%. In addition to the set size reduction, the produced classes are semantically consistent with the predicted agent classes: large vehicle and Bus. More qualitative examples are presented in Appendix D.

lation [16], human-robot interaction [17, 18], autonomous perception [19, 20, 21], and autonomous navigation [22, 23].

The separate application of traditional CP to different tasks does not guarantee semantic consistency. In our context, semantic consistency refers to the logical alignment of predictions across different tasks, ensuring that the inferred attributes are contextually appropriate and mutually compatible. To illustrate this, we present in Figure 1b the result of one of our experiments on the ROAD dataset [1], where an autonomous agent uses three distinct models to classify an agent, its location, and its action. Applying traditional CP to each task in isolation results in high uncertainty and low semantic consistency. High uncertainty is shown by the numerous potential classes of actions and locations. Low semantic consistency is seen in the conflicting locations (e.g., *incoming cycle lane*) and actions (e.g., *crossing*) for the agent classes (i.e., *large vehicle* and *bus*). It is important to note that simply removing inconsistent classes compromises CP coverage guarantees, which is undesirable.

In this work, we address the construction of conformal prediction sets across various classification tasks for perception, such as agent, action, and location classification, while ensuring conformal prediction validity and semantic consistency among the produced sets for each task. We propose Knowledge-Refined Prediction Sets (KRPS), a novel CP approach that reduces uncertainty in autonomous agents in urban environments by producing valid, uncertainty-aware prediction sets that are semantically consistent across multiple tasks. KRPS consists of a knowledge graph that links the different tasks, and a sequential[1] set construction procedure based on an intial task to ensure the produced sets for subsequent tasks cover the true label with a user-defined probability. The sequential processing of tasks in KRPS allows for efficient on-demand refinement of subsequent task predictions, based on initial task results. As depicted in Figure 1c, KRPS sequentially refines the prediction sets for the location and action tasks using the prediction sets from the agent classification task and a knowledge graph. In this case, KRPS leads to more semantically consistent results, reflected by the alignment between the agent classes, its possible locations, and actions, and leads to 80% lower uncertainty when compared to traditional CP, reflected by the lower number of classes in the prediction sets. In cases where the knowledge graph is incomplete, KRPS manages corner cases, such as anomalies where vehicles are located on sidewalks, by outputting empty prediction sets, indicating the absence of semantically consistent labels. We provide a theoretical analysis of KRPS, introducing the concept of conditional semantic consistency for multitask-based autonomous perception and demonstrating the semantic consistency and marginal coverage properties of the produced sets. We evaluate KRPS on 2 large-scale autonomous driving datasets, namely the ROAD dataset [1] and Waymo/ROAD++ dataset [24], from the scope of 3 high-level perception tasks that are crucial for semantically-aware autonomous perception and high-level reasoning in urban settings: object class, location, and action. The results of our evaluation show that KRPS outperforms state-of-the-art conformal prediction approaches in reducing the uncertainty of the models by up to 80% and increasing the semantic consistency by up to 30%, through the generation of smaller prediction sets that are semantically consistent through the tasks while holding the coverage guarantees.

[1] Sequentiality in our context means refining predictions for one task at a time.

2 Background on Conformal Prediction

We focus on CP for classification, as it is the relevant task for our work. Let g_θ be a classifier pre-trained on a dataset D_{train}. The model g_θ outputs estimated probabilities for each class (e.g., softmax scores), such that $g_\theta(X) \in [0,1]^K$, where X is an input image and K is the number of classes considered.

Assumption. CP assumes the existence of *exchangeable* unseen pairs of data examples that are drawn from the same data distribution as D_{train}, to which we refer to as calibration set D_{cal}. The goal of CP is to construct prediction sets for unseen data samples $C(X_{test})$ that are valid, i.e., they contain the true label Y_{test} with a probability $1-\alpha$, where α is a user-defined error rate. This property is called *marginal coverage* and is expressed in Equation 1.

$$\mathbb{P}[Y_{test} \in C(X_{test})] \geq 1-\alpha \tag{1}$$

To construct the prediction sets, CP requires a test statistic called *non-conformity score* $S(X,Y)$, which measures the dissimilarity between predictions generated for an unseen data point and the training data. Based on S, the elements of D_{cal} are ranked, and the empirical $1-\alpha$ quantile $\hat{q}$ is calculated. For a novel X_{test}, for which Y_{test} is unknown at test time, $C(X_{test})$ is constructed as $C(X_{test}) = \{Y : S(X,Y) \leq \hat{q}\}$. This procedure can be expressed through p-values that measure the probability of non-conformity, as formalized in Theorem 2.1.

Theorem 2.1 (Conformal Prediction [10]) *Let D_{train}, D_{cal}, and X_{test} be sets of exchangeable random variables. Let S be a non-conformity score and α be a user-defined error rate. The set $C(X_{test})$ defined as $C(X_{test}) = \{Y \in \mathcal{Y} : p\text{-}value(S(X_{test}, Y)) \geq \alpha\}$ satisfies the marginal coverage property stated in Equation 1.*

3 Knowledge-Refined Prediction Sets

We address the problem of autonomous perception for urban scene understanding based on the reasoning across multiple high-level tasks, that allow the agent to make uncertainty-aware and semantically consistent predictions. We focus on 3 classification tasks: agent type, agent location, and agent action, that are deemed necessary to achieve a high-level semantic understanding of the robot's environment [1, 2, 3, 4]. We assume the existence of 3 separate neural networks g^c, g^l, and g^a that output the agent class $\hat{Y}^c_j \in \mathcal{Y}^c$, agent location class $\hat{Y}^l_j \in \mathcal{Y}^l$, and agent action class $\hat{Y}^a_j \in \mathcal{Y}^a$, respectively, given a bounding box around the agent of interest X_j, where $X_j \in \mathcal{X}$, and $\mathcal{X}$ represents the set of all agents of interest in a scene. Given the models g^c, g^l, and g^a, a calibration set D_{cal}, and an unseen test sample X_{test}, our goal is to sequentially construct the prediction sets $C_l(X_{test})$ for location classification, and $C_a(X_{test})$ for action classification, given a $C_c(X_{test})$ that was generated by an agent classification CP algorithm. We opt for sequential task refinement as it permits on-demand processing of subsequent tasks in case of need. We desire our generated sets to have two properties. The first property is marginal coverage as described in Equation 1, which means that the predicted sets are guaranteed to include the true label Y_{test} with a probability of at least $1-\alpha$. The second property is semantic consistency, which means that the prediction sets for each of the classification tasks need to account for classes included in other sets. For example, for $C_c(X_{test}) = \{\text{car, medium vehicle, large vehicle}\}$ it is clear that Y_{test} corresponds to a vehicle, and so $C_l(X_{test})$ should not include locations that are not proper to vehicles, such as *sidewalk*. Traditional CP set-ups do not guarantee these properties, as they only consider one task. In this work, we propose knowledge-refined prediction sets (KRPS), a CP-based approach that constructs the prediction sets described above given an initial task and a knowledge graph. For the remainder of this paper, we refer to sets constructed by KRPS by $C^{KRPS}_c(X_{test})$, $C^{KRPS}_l(X_{test})$, and $C^{KRPS}_a(X_{test})$.

KRPS consists of two components: a knowledge graph and a knowledge-based multitask conformal prediction algorithm. The knowledge graph models the semantic relationships between the different tasks we consider. For a particular agent class, only a subset of all possible locations and actions can be assigned. The other component of our approach is the knowledge-refined multitask conformal prediction algorithm that leverages the knowledge graph to sequentially construct prediction sets for each task, that are semantically consistent while satisfying the coverage guarantees. The semantic consistency is ensured through a knowledge-based pruning procedure that removes location and action classes if they are semantically inconsistent with the agent class.

Knowledge Graph Construction. To construct knowledge-refined prediction sets (KRPS), we build a knowledge graph $\mathcal{K}$ in order to model the semantic relationships between the tasks. The knowledge graph in our implementation draws from common sense and available labels in large-scale datasets for urban scene understanding, such as the ROAD and Waymo/ROAD++ datasets [1, 24], as we detail in Appendix B. Using the labels for each task, the semantic relationships between the tasks are constructed as follows. Given a task $\mathcal{T}_c$ and $\mathcal{T}_a$ referring to the tasks of agent classification and agent action classification, $\mathcal{K}$ contains a set-valued deterministic function $\mathcal{M}_{c \to a} : \mathcal{Y}^c \to 2^{\mathcal{Y}^a}$ that maps agent class labels to the set of all possible action labels, as it is depicted in Figure 2a. Figure 2b shows an example of this mapping, where the class cyclist is mapped to all its possible locations by $\mathcal{M}_{c \to l}$, and to all its possible actions by $\mathcal{M}_{c \to a}$. Given $\mathcal{K}$, we introduce the notion of conditional semantic consistency between prediction sets for each task.

Definition 3.1 (Conditional Semantic Consistency) *Let C_j and C_i be 2 prediction sets containing class candidates for the tasks $\mathcal{T}^j$ and $\mathcal{T}^i$, respectively. C_i is semantically consistent **with respect to** C_j and $\mathcal{K}$, if:*

$$\forall Y_i \in C_i, \exists Y_j \in C_j | Y_j \in \mathcal{M}_{i \to j}(Y_i) \tag{2}$$

Equation 2 implies that every element in C_i has a pre-image in C_j by the semantic mapping $\mathcal{M}_{i \to j}$. Note that with this definition, C_j can have elements that do not have images in C_i.

KRPS Construction Procedure. KRPS is based on sequentially pruning prediction sets using knowledge from $\mathcal{K}$. For a given scene and an object X_{test}, we start by constructing the prediction set for the agent class task $C_c^{KRPS}(X_{test})$. Since our approach is sequential, the construction procedure of the prediction set for the first task follows the usual CP procedure based on Theorem 2.1. Next, we acquire all possible locations of agent classes in $C_c^{KRPS}(X_{test})$ using the semantic mapping from the knowledge graph $\mathcal{K}$. The set of all possible locations that correspond to $C_c^{KRPS}(X_{test})$ is $C_l^{\mathcal{K}} = \mathcal{M}_{c \to l}(C_c^{KRPS})$[2]. We use $C_l^{\mathcal{K}}$ as a starting set for further pruning, instead of considering the full space of labels $\mathcal{Y}^l$. The pruning consists of a conformal prediction step based on a conformity score proper to the location classification task. Examples of such conformity scores are $1 - Softmax$. The conformal prediction step produces the set C_l^{KRPS}. Applying the steps described above results in a multi-hypotheses testing problem, where the family-wise error increases. To account for the MHT problem, applying a correction procedure M of the p-values is required, as we detail in Appendix A. Prediction sets for further tasks can be acquired by applying the same procedure sequentially using C_l^{KRPS}. Using the procedure explained above, the generated sets are guaranteed to be semantically consistent and to have coverage as formalized in Equation 1. The KRPS set construction proce-

Algorithm 1: KRPS Procedure

```
Input  : $\mathcal{K}$: knowledge graph.
         $\mathcal{T}_1..\mathcal{T}_m$: set of tasks.
         $\mathcal{M}_{\mathcal{T}_i \to \mathcal{T}_{i+1}}$, semantic mappings.
         $M$: correction procedure.
         $D_{cal}$: calibration set.
         $\alpha$: user-defined error rate.
Output: $C_{\mathcal{T}_i}^{KRPS}, i \in [1, m]$: semantically
         consistent prediction sets.
$C_{\mathcal{T}_0}^{KRPS} \leftarrow \cdot \mathcal{Y}^0$
$P_{\mathcal{T}_i} \leftarrow 1, \forall Y^{\mathcal{T}_i} \in \mathcal{Y}^{\mathcal{T}_i}, i \in [0, m]$
for $i = 1$ to $m$ do
    $C_{\mathcal{T}_i}^{\mathcal{K}} \leftarrow \cdot \mathcal{M}_{\mathcal{T}_{i-1} \to \mathcal{T}_i}(C_{\mathcal{T}_{i-1}}^{KRPS})$
    $C_{\mathcal{T}_i}^{KRPS} \leftarrow \{\}$
    for $y \in C_{\mathcal{T}_i}^{\mathcal{K}}$ do
        $P_{\mathcal{T}_i} \leftarrow$M(p-value(X$_{test}$, $D_{cal}$))
        if $P_{\mathcal{T}_i} \geq \alpha$ then
            $C_{\mathcal{T}_i}^{KRPS} \leftarrow$ C$_{\mathcal{T}_i}^{KRPS} \cup \{y\}$
    end for
end for
return $C_{\mathcal{T}_i}^{KRPS}, i \in [1, m]$
```

[2] $\mathcal{M}_{c \to l}$ is a point to set mapping. We abuse the notation to indicate the set of images for every elements in C_c^{KRPS} using the mapping $\mathcal{M}_{c \to l}$.

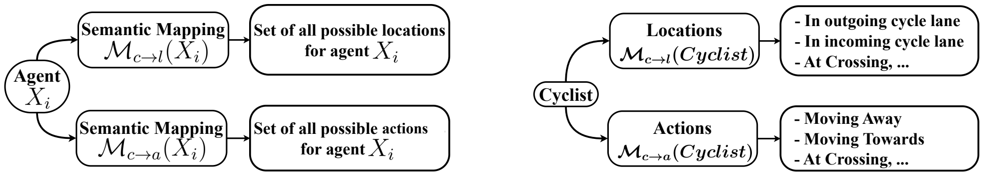
Semantic Mapping
$\mathcal{M}_{c\to l}(X_i)$
Set of all possible locations for agent X_i
Agent
X_i
Semantic Mapping
$\mathcal{M}_{c\to a}(X_i)$
Set of all possible actions for agent X_i
Locations
$\mathcal{M}_{c\to l}(Cyclist)$
- In outgoing cycle lane
- In incoming cycle lane
- At Crossing, ...
Cyclist
Actions
$\mathcal{M}_{c\to a}(Cyclist)$
- Moving Away
- Moving Towards
- At Crossing, ...

(a) General structure of the knowledge graph.

(b) Knowledge graph for the agent class *Cyclist*.

Figure 2: Knowledge-graph structure used in KRPS. Figure 2a shows the structure of the knowledge graph with the semantic mappings $\{agent \rightarrow location\}$ and $\{agent \rightarrow action\}$. Figure 2b depicts an example graph for the agent class *Cyclist*. The full construction procedure is in Appendix B.

dure is formalized in Theorem 3.1 and described in Algorithm 1. The proof of Theorem 3.1 and its corollary, along with an analysis of their practical implications, are provided in Appendix A.

Theorem 3.1 (Knowledge-Refined Conformal Prediction) *Given 2 tasks $\mathcal{T}_c$ and $\mathcal{T}_l$, the semantic mapping function $\mathcal{M}_{c\rightarrow l}$, and the prediction sets $C^c(X_{test})$ and $C^l(X_{test})$, the set $C_l^{KRPS}(X_{test}) = C^l(X_{test}) \cap \mathcal{M}_{c\rightarrow l}(Y^c_{test})$ is* ***semantically consistent*** *with respect to C_c^{KRPS} and $\mathcal{K}$, and satisfies the* ***marginal coverage*** *described in Equation 3.*

$$\mathbb{P}[Y_{test} \in C_l^{KRPS}(X_{test})] \geq 1 - \alpha \tag{3}$$

We prove this property by leveraging the probability conservation of the deterministic semantic mappings between the task and proposing a generalizing of the cascaded CP Theorem [25] to cover multitask settings. We present the detailed proof of Theorem 3.1 in Appendix A.

Corollary 3.1 (Transitivity of conditional semantic consistency) *Let C_c^{KRPS}, C_l^{KRPS} and C_a^{KRPS} be 3 prediction sets constructed using KRPS. If C_l^{KRPS} is semantically consistent, with respect to C_c^{KRPS} and $\mathcal{K}$, and C_a^{KRPS} is semantically consistent, with respect to C_l^{KRPS} and $\mathcal{K}$, then and C_a^{KRPS} is semantically consistent, with respect to C_c^{KRPS} and $\mathcal{K}$.*

We prove the transitivity property by leveraging the semantic consistency between prediction sets of subsequent tasks, guaranteed by Theorem 3.1. We present a proof of Corollary 3.1 in Appendix A.

4 Evaluation

To support the theoretical results for guaranteed coverage and semantic consistency across different tasks executed sequentially, we evaluate KRPS on 2 large-scale urban scene understanding datasets. We compare the performance of KRPS against 3 baselines including 2 state-of-the-art approaches, using 2 widely used CP metrics: deviation from coverage rate and set size. Since we are the first to consider semantic consistency across tasks in CP, we introduce a metric for semantic consistency.

4.1 Datasets

The ROAD Dataset [1]. The Road Event Awareness dataset (ROAD) for autonomous driving includes 22 videos, and 1.7M labels across 11 agent classes, 15 locations, and 23 actions under various weather conditions, providing a diverse and challenging set of scenarios for testing the effectiveness of KRPS. ROAD offers (agent, location, action) triplets, ideal for a comprehensive evaluation.

The Waymo/ROAD++ Dataset[3]. The Waymo/ROAD++ dataset, an extension of the ROAD dataset, incorporates 3.5M agents, 4.3M actions, and 4.2M locations from the expansive Waymo autonomous driving dataset [24], annotated with road events akin to those in the ROAD dataset.

Implementation. For the evaluation, we use the 3D-RetinaNet [1] with separate heads for each classification task, outputting softmax scores. The model is trained on each dataset for 30 epochs

[3] Waymo/ROAD++: https://sites.google.com/view/road-plus-plus/dataset

with an Adam optimizer at a learning rate of $lr = 0.001$. We randomly divide the validation splits of both datasets in 3 equal-sized portions as follows: *eval split 1* for validation, *eval split 2* for calibration, and *eval split 3* for testing. All experiments use Bonferroni correction for prediction robustness, with results averaged over 100 trials on a single 24GB RTX 3090.[4]

4.2 Metrics

Deviation from Target Coverage (DTC). The deviation from the target coverage rate (DTC) quantifies the discrepancy between the achieved coverage, $Cov_{approach}$, and the desired target coverage, $Cov_{target} = 1 - \alpha$, as defined in Equation 4.

$$DTC = Cov_{approach} - Cov_{target} \tag{4}$$

Negative DTC values indicate coverage below $1 - \alpha$, indicating a failure to meet the theoretical lower bound. DTC values nearing zero suggest that the actual coverage closely aligns with the target coverage. **Smaller positive** values denote accurate coverage rates above the desired threshold.

Set Size (SS). We measure the average set size provided by KRPS. As providing the full set of labels would be a trivial output for CP-based methods to achieve the coverage guarantees, a smaller set size demonstrates better predictive efficiency.

Conditional Semantic Consistency (SC). We introduce a novel metric to measure the semantic consistency between the generated sets predicted for the task $\mathcal{T}^i$ with respect to $\mathcal{T}^{i-1}$ and $\mathcal{K}$. For a prediction set $C_{\mathcal{T}^i}$, semantic consistency represents the rate of semantically consistent classes in the entire set and is formulated in Equation 5. A higher semantic consistency value demonstrates better coherence between the prediction sets across the tasks.

$$SC(C_{\mathcal{T}^i} | C_{\mathcal{T}^{i-1}}, \mathcal{K}) = \frac{|\{Y : Y \in C_{\mathcal{T}^i} \cap \mathcal{M}_{\mathcal{T}_{i-1} \to \mathcal{T}_i}(C_{\mathcal{T}_{i-1}})\}|}{|C_{\mathcal{T}^i}|} \tag{5}$$

4.3 Baselines

Inspired by recent CP works, such as [26, 25], we evaluate KRPS with the Least Ambiguous Set Classifier (LAC), for which the scoring function is $1 - Softmax$ [27], and 2 state-of-the-art CP scores. The first approach is adaptive predictive sets (APS) [28], which is a scoring technique known to improve conditional coverage. The second approach is regularized adaptive predictive sets (RAPS) [29], which is known to generate notably smaller predictive sets. RAPS stands unparalleled in minimizing the size of prediction sets. Thus, it is crucial to explore the effectiveness of KRPS in further compressing the predictive set sizes relative to those generated by RAPS.

4.4 Tasks

Our evaluation considers 3 tasks on both datasets, namely agent, location, and action classification. Since our approach acts sequentially on multiple tasks, the first task is not refined, which makes the construction of the prediction set for the first task (i.e., agent classification), coincide with the underlying CP process. The task sequences we consider are: $\{agent \to location\}$ and $\{agent \to action\}$. To conduct our evaluation, we first construct the prediction sets for the agent classification using $Softmax$, APS, and RAPS. Using the predicted agent class sets, we report the results for the subsequent tasks: location classification, and action classification. In Appendix C, We report the results of longer task sequences using 3 tasks to show the capability to handle longer sequences of tasks with different orders.

4.5 Comparison with State-of-the-Art

We conduct our evaluation using different values of α ranging from 0.1 to 0.5 with a step of 0.1. We present the results on the ROAD and Waymo/ROAD++ datasets in Table 1a and Table 1b, re-

[4] Our code is available here: https://gitlab.com/achref.d/krps.

Task	Score	Method	$\alpha = 0.1$			$\alpha = 0.2$			$\alpha = 0.4$		
			SS	DTC	SC	SS	DTC	SC	SS	DTC	SC
Location	Softmax	Standard	7.07	0.05	0.81	6.04	0.10	0.79	4.51	0.19	0.77
		KRPS	**5.86**	**0.02**	**1.00**	**4.93**	**0.05**	**1.00**	**3.75**	**0.09**	**1.00**
	APS	Standard	7.12	0.05	0.80	6.07	0.10	0.79	4.61	0.20	0.76
		KRPS	**5.90**	**0.02**	**1.00**	**4.96**	**0.05**	**1.00**	**3.65**	**0.12**	**1.00**
	RAPS	Standard	2.66	0.07	0.89	2.03	0.15	0.93	1.56	0.34	0.96
		KRPS	**2.18**	**0.05**	**1.00**	**1.78**	**0.13**	**1.00**	**1.45**	**0.13**	**1.00**
Action	Softmax	Standard	7.48	0.01	0.79	5.98	0.01	0.78	3.77	0.06	0.77
		KRPS	**5.83**	**0.00**	**1.00**	**4.70**	**0.00**	**1.00**	**3.06**	**0.00**	**1.00**
	APS	Standard	9.77	0.05	0.75	8.01	0.10	0.73	5.72	0.30	0.70
		KRPS	**7.29**	**0.02**	**1.00**	**6.01**	**0.03**	**1.00**	**4.35**	**0.11**	**1.00**
	RAPS	Standard	4.67	0.07	0.84	3.94	0.13	0.87	2.54	0.25	0.92
		KRPS	**3.82**	**0.03**	**1.00**	**3.26**	**0.02**	**1.00**	**2.22**	**0.15**	**1.00**

(a) Results on the ROAD dataset for for $\alpha = [0.1, 0.2, 0.4]$. **Bold** designates better performance.

Task	Score	Method	$\alpha = 0.1$			$\alpha = 0.2$			$\alpha = 0.4$		
			SS	DTC	SC	SS	DTC	SC	SS	DTC	SC
Location	Softmax	Standard	8.10	0.05	0.80	6.04	0.11	0.73	4.13	0.21	0.72
		KRPS	**6.02**	**0.01**	**1.00**	**5.42**	**0.03**	**1.00**	**3.07**	**0.08**	**1.00**
	APS	Standard	9.02	0.07	0.79	7.92	0.10	0.76	4.03	0.22	0.71
		KRPS	**7.50**	**0.01**	**1.00**	**5.99**	**0.06**	**1.00**	**3.24**	**0.14**	**1.00**
	RAPS	Standard	2.45	0.09	0.87	2.07	0.15	0.91	1.83	0.34	0.96
		KRPS	**2.01**	**0.04**	**1.00**	**2.04**	**0.10**	**1.00**	**1.17**	**0.09**	**1.00**
Action	Softmax	Standard	9.32	0.06	0.80	7.20	0.08	0.78	5.00	0.15	0.81
		KRPS	**6.09**	**0.01**	**1.00**	**4.17**	**0.03**	**1.00**	**3.50**	**0.10**	**1.00**
	APS	Standard	10.41	0.05	0.77	6.84	0.13	0.74	5.36	0.12	0.78
		KRPS	**5.98**	**0.02**	**1.00**	**4.18**	**0.02**	**1.00**	**3.87**	**0.12**	**1.00**
	RAPS	Standard	4.36	0.06	0.87	3.03	0.15	0.89	1.50	0.24	0.94
		KRPS	**3.57**	**0.04**	**1.00**	**2.88**	**0.02**	**1.00**	**1.07**	**0.07**	**1.00**

(b) Results on the Waymo/ROAD++ dataset for for $\alpha = [0.1, 0.2, 0.4]$. **Bold** designates better performance.

Table 1: Results of our experiments. Based on the prediction sets for the agent classification task, prediction sets for the location and action are sequentially inferred using KRPS with 3 scoring functions: $Softmax$, APS, and RAPS. The standard mode refers to the baseline without KRPS.

spectively. Due to space constraints, we only report the results for $\alpha = [0.1, 0.2, 0.4]$, in the main manuscript. Results for the full set of α values and different task sequences are in Appendix C.

The results show that KRPS substantially reduces the set size for all underlying scores. For the location classification task, the average set size reduction is by 17% for softmax, 18% for APS, and 10% for RAPS, for the ROAD dataset, and by 20% for softmax, 20% for APS, and 27% for RAPS, for the ROAD++ dataset. For the action classification task, the set size reduction achieved by KRPS is more apparent and equals 24% for softmax, 25% for APS, and 16% for RAPS, for the ROAD dataset. For the Waymo/ROAD++ dataset, the results show that KRPS achieved a set size reduction by 36% for softmax, 38% for APS, and 15.4% for RAPS. The contribution of KRPS to set size reduction is particularly apparent for APS, in both datasets. The reason is that APS is built to achieve class-wise coverage to account for unbalanced classes in the dataset, which has the effect of increasing the set size. The application of KRPS succeeds in reducing the set size while holding the marginal coverage guarantees. KRPS holds the theoretical coverage guarantees for all values of α and for all the non-conformity scores, which is indicated by positive DTC values. Furthermore, KRPS adjusts the coverage rate for all scoring functions, leading to lower DTC values.

KRPS holds conditional semantic consistency guarantees as well, achieving 100% of conditional semantic consistency in all experimental conditions. Compared to the baselines, KRPS increases the conditional semantic consistency in the task of location classification by an average of 26% for softmax, 23% for APS, and 6% for RAPS, for the ROAD dataset, and by 26% for softmax, 23% for APS, and 6% for RAPS, for the ROAD++ dataset. For the task of action classification on the ROAD dataset, KRPS increased the semantic consistency by 25% for softmax, 24% for APS, and 8% for RAPS. For the Waymo/ROAD++ dataset as well, KRPS increases the semantic consistency rates for action prediction by 25.5% for softmax, 31% for APS, and 11% for RAPS. We present more experiments on longer task sequences, the influence of the knowledge graph size, and the percentage of the empty sets in Appendices B, and E, respectively.

5 Discussion

Recent studies have underscored the importance of incorporating semantics [30, 31, 32, 33] and uncertainty [34, 35, 36, 37] into robotic decision-making frameworks, particularly as Large Language Models (LLMs) are increasingly used to enhance autonomous navigation [38, 39, 40, 41]. These models, prone to uncertainty and hallucinations [42], necessitate a detailed contextual understanding of the scene for effective operation [43]. Incorporating semantic awareness and uncertainty awareness enhances both the reliability and interpretability of these systems, addressing a fundamental challenge in their widespread adoption: trust [44, 45]. KRPS introduces a novel approach that combines these aspects to improve the overall efficacy of autonomous decision-making processes. KRPS represents the first approach that extends CP to a multitask learning setup without specific requirements regarding the nature or sequencing of tasks. The theoretical analysis and the empirical evaluation show that KRPS significantly reduces uncertainty, while ensuring semantic consistency, in dynamic urban environments. Furthermore, KRPS benefits from the inherent practicalities of CP, eliminating the need for continual model retraining. Instead, KRPS requires only a computationally efficient calibration process to integrate new data, assuming data exchangeability as per CP norms.

Limitations. As we see KRPS as a practical approach to consider uncertainty and semantic awareness in autonomous robots and systems, it is important to consider the limitations of its application. KRPS, being a CP-based approach, traditionally relies on the assumption of data exchangeability. This assumption can limit its effectiveness with scoring functions that fail to address out-of-distribution (OOD) data scenarios. To mitigate this, KRPS has been designed to be agnostic to the scoring function, as demonstrated in our empirical analysis, making it compatible with OOD-aware calibration procedures, such as [46, 47, 12]. The effectiveness of KRPS is also contingent on the integrity of the underlying knowledge graph. Ambiguities within the knowledge graph regarding class definitions can compromise prediction accuracy. To address this, our evaluation integrates ontological structures derived from the datasets utilized, such as ROAD and Waymo [1, 24], and aligns with established logical frameworks [2], facilitating more precise semantic interpretations. Moreover, KRPS is designed to identify and respond to these ambiguities by generating empty prediction sets to effectively manage scenarios not fully covered by the knowledge graph. This feature highlights cases requiring further scrutiny and ensures that KRPS maintains reliability despite incomplete ontologies. KRPS is a sequential approach, leveraging prediction sets from the initial task to generate semantically consistent sets for subsequent tasks. Its dependence on the quality of the first set is intrinsic. Although joint prediction set construction is viable [48], the sequential process allows for on-demand refinements exclusively for the relevant agents in the scene, leading to better efficiency.

Practicality. While our paper focuses on 3 high-level perception tasks for urban scene understanding, KRPS can be extended to other robot perception applications. The formulation of Algorithm 1 and Theorem 3.1 is adaptable to diverse environmental contexts. For example, KRPS can be applied to urban search and rescue, handling sequences of tasks under high uncertainty like victim detection, hazard identification, and robot action selection. Other use-cases can also be envisioned, such as robot manipulation, where a robot is tasked to recognize and sort objects of different sizes and put them in their corresponding places. KRPS provides uncertainty quantification and semantic consistency at each stage, ensuring accurate object classification, optimal grasp strategy selection, and precise object placement. We elaborate more on these applications in Appendix F.

6 Conclusion

We introduced KRPS, a Knowledge-Refined Prediction Set approach, tailored for multitask learning in urban scene understanding. By refining prediction sets through semantic relationships among tasks, KRPS ensures semantic consistency and adheres to coverage guarantees by producing significantly smaller prediction sets. KRPS shows promise for real-world applications, particularly in autonomous driving. Due to safety concerns, initial tests were limited to realistic, and challenging datasets. Future work should focus on integrating KRPS into operational systems, with rigorous safety validations and controlled real-world trials to ensure trustworthy autonomous navigation.

Acknowledgments

This work has been partially funded by the German Federal Ministry of Education and Research (BMBF) through the Software Campus Program.

References

[1] G. Singh, S. Akrigg, M. Di Maio, V. Fontana, R. J. Alitappeh, S. Khan, S. Saha, K. Jeddisaravi, F. Yousefi, J. Culley, et al. Road: The road event awareness dataset for autonomous driving. *IEEE transactions on pattern analysis and machine intelligence*, 45(1):1036–1054, 2022.

[2] E. Giunchiglia, M. C. Stoian, S. Khan, F. Cuzzolin, and T. Lukasiewicz. Road-r: The autonomous driving dataset with logical requirements. *Machine Learning*, pages 1–31, 2023.

[3] S. Malla, C. Choi, I. Dwivedi, J. H. Choi, and J. Li. Drama: Joint risk localization and captioning in driving. In *Proceedings of the IEEE/CVF Winter Conference on Applications of Computer Vision*, pages 1043–1052, 2023.

[4] E. Sachdeva, N. Agarwal, S. Chundi, S. Roelofs, J. Li, M. Kochenderfer, C. Choi, and B. Dariush. Rank2tell: A multimodal driving dataset for joint importance ranking and reasoning. In *Proceedings of the IEEE/CVF Winter Conference on Applications of Computer Vision*, pages 7513–7522, 2024.

[5] B. Wilson, W. Qi, T. Agarwal, J. Lambert, J. Singh, S. Khandelwal, B. Pan, R. Kumar, A. Hartnett, J. K. Pontes, D. Ramanan, P. Carr, and J. Hays. Argoverse 2: Next generation datasets for self-driving perception and forecasting. In *Proceedings of the Neural Information Processing Systems Track on Datasets and Benchmarks (NeurIPS Datasets and Benchmarks 2021)*, 2021.

[6] P. Kochakarn, D. De Martini, D. Omeiza, and L. Kunze. Explainable action prediction through self-supervision on scene graphs. In *2023 IEEE International Conference on Robotics and Automation (ICRA)*, pages 1479–1485. IEEE, 2023.

[7] D. Omeiza, S. Anjomshoae, H. Webb, M. Jirotka, and L. Kunze. From spoken thoughts to automated driving commentary: Predicting and explaining intelligent vehicles' actions. In *2022 IEEE Intelligent Vehicles Symposium (IV)*, pages 1040–1047. IEEE, 2022.

[8] R. Wickramarachchi, C. Henson, and A. Sheth. An evaluation of knowledge graph embeddings for autonomous driving data: Experience and practice. *arXiv preprint arXiv:2003.00344*, 2020.

[9] A. Zareian, S. Karaman, and S.-F. Chang. Bridging knowledge graphs to generate scene graphs. In *Computer Vision–ECCV 2020: 16th European Conference, Glasgow, UK, August 23–28, 2020, Proceedings, Part XXIII 16*, pages 606–623. Springer, 2020.

[10] V. Vovk, A. Gammerman, and G. Shafer. *Algorithmic Learning in a Random World*. Springer-Verlag, Berlin, Heidelberg, 2005. ISBN 0387001522.

[11] G. Shafer and V. Vovk. A tutorial on conformal prediction. *Journal of Machine Learning Research*, 9(3), 2008.

[12] A. N. Angelopoulos and S. Bates. A gentle introduction to conformal prediction and distribution-free uncertainty quantification. *arXiv preprint arXiv:2107.07511*, 2021.

[13] L. Gan, Y. Kim, J. W. Grizzle, J. M. Walls, A. Kim, R. M. Eustice, and M. Ghaffari. Multitask learning for scalable and dense multilayer bayesian map inference. *IEEE Transactions on Robotics*, 39(1):699–717, 2022.

[14] W. Zhou, T. Gong, J. Lei, and L. Yu. Dbcnet: Dynamic bilateral cross-fusion network for rgb-t urban scene understanding in intelligent vehicles. *IEEE Transactions on Systems, Man, and Cybernetics: Systems*, 2023.

[15] K. Sirohi, S. Marvi, D. Büscher, and W. Burgard. Uncertainty-aware panoptic segmentation. *IEEE Robotics and Automation Letters*, 8(5):2629–2636, 2023.

[16] J. Sun, Y. Jiang, J. Qiu, P. Nobel, M. J. Kochenderfer, and M. Schwager. Conformal prediction for uncertainty-aware planning with diffusion dynamics model. *Advances in Neural Information Processing Systems*, 36, 2024.

[17] J. Lidard, H. Pham, A. Bachman, B. Boateng, and A. Majumdar. Risk-calibrated human-robot interaction via set-valued intent prediction. In *ICRA 2024 Workshop {\textemdash} Back to the Future: Robot Learning Going Probabilistic*.

[18] A. Z. Ren, A. Dixit, A. Bodrova, S. Singh, S. Tu, N. Brown, P. Xu, L. Takayama, F. Xia, J. Varley, et al. Robots that ask for help: Uncertainty alignment for large language model planners. In *Conference on Robot Learning*, pages 661–682. PMLR, 2023.

[19] Y. Zhang, S. Wang, Y. Zhang, and D. Z. Chen. Rr-cp: Reliable-region-based conformal prediction for trustworthy medical image classification. In *International Workshop on Uncertainty for Safe Utilization of Machine Learning in Medical Imaging*, pages 12–21. Springer, 2023.

[20] A. Fisch, T. Schuster, T. Jaakkola, and R. Barzilay. Few-shot conformal prediction with auxiliary tasks. In *International Conference on Machine Learning*, pages 3329–3339. PMLR, 2021.

[21] J. Teng, C. Wen, D. Zhang, Y. Bengio, Y. Gao, and Y. Yuan. Predictive inference with feature conformal prediction. *11th International Conference on Learning Representations, ICLR 2023*, 2023.

[22] L. Lindemann, M. Cleaveland, G. Shim, and G. J. Pappas. Safe planning in dynamic environments using conformal prediction. *IEEE Robotics and Automation Letters*, 2023.

[23] A. Dixit, L. Lindemann, S. X. Wei, M. Cleaveland, G. J. Pappas, and J. W. Burdick. Adaptive conformal prediction for motion planning among dynamic agents. In *Learning for Dynamics and Control Conference*, pages 300–314. PMLR, 2023.

[24] P. Sun, H. Kretzschmar, X. Dotiwalla, A. Chouard, V. Patnaik, P. Tsui, J. Guo, Y. Zhou, Y. Chai, B. Caine, et al. Scalability in perception for autonomous driving: Waymo open dataset. In *Proceedings of the IEEE/CVF conference on computer vision and pattern recognition*, pages 2446–2454, 2020.

[25] A. Fisch, T. Schuster, T. S. Jaakkola, and R. Barzilay. Efficient conformal prediction via cascaded inference with expanded admission. In *9th International Conference on Learning Representations, ICLR 2021, Virtual Event, Austria, May 3-7, 2021*.

[26] T. Ding, A. Angelopoulos, S. Bates, M. Jordan, and R. J. Tibshirani. Class-conditional conformal prediction with many classes. *Advances in Neural Information Processing Systems*, 36, 2024.

[27] M. Sadinle, J. Lei, and L. Wasserman. Least ambiguous set-valued classifiers with bounded error levels. *Journal of the American Statistical Association*, 114(525):223–234, 2019.

[28] Y. Romano, M. Sesia, and E. Candes. Classification with valid and adaptive coverage. *Advances in Neural Information Processing Systems*, 33:3581–3591, 2020.

[29] A. N. Angelopoulos, S. Bates, M. I. Jordan, and J. Malik. Uncertainty sets for image classifiers using conformal prediction. In *9th International Conference on Learning Representations, ICLR 2021, Virtual Event, Austria, May 3-7, 2021*, 2021.

[30] C. Russo, K. Madani, and A. M. Rinaldi. Knowledge acquisition and design using semantics and perception: a case study for autonomous robots. *Neural Processing Letters*, 53(5):3153–3168, 2021.

[31] B. Yu, H. Kasaei, and M. Cao. Co-navgpt: Multi-robot cooperative visual semantic navigation using large language models. *arXiv preprint arXiv:2310.07937*, 2023.

[32] C. Tang, D. Huang, W. Ge, W. Liu, and H. Zhang. Graspgpt: Leveraging semantic knowledge from a large language model for task-oriented grasping. *IEEE Robotics and Automation Letters*, 2023.

[33] Y. Feng, W. Hua, and Y. Sun. Nle-dm: Natural-language explanations for decision making of autonomous driving based on semantic scene understanding. *IEEE Transactions on Intelligent Transportation Systems*, 2023.

[34] R. Michelmore, M. Wicker, L. Laurenti, L. Cardelli, Y. Gal, and M. Kwiatkowska. Uncertainty quantification with statistical guarantees in end-to-end autonomous driving control. In *2020 IEEE international conference on robotics and automation (ICRA)*, pages 7344–7350. IEEE, 2020.

[35] N. Shah and S. Srivastava. Zero-shot option invention for robot planning under uncertainty. In *CoRL 2023 Workshop on Learning Effective Abstractions for Planning (LEAP)*, 2023.

[36] X. Tang, K. Yang, H. Wang, J. Wu, Y. Qin, W. Yu, and D. Cao. Prediction-uncertainty-aware decision-making for autonomous vehicles. *IEEE Transactions on Intelligent Vehicles*, 7(4): 849–862, 2022.

[37] X. He, W. Huang, and C. Lv. Toward trustworthy decision-making for autonomous vehicles: A robust reinforcement learning approach with safety guarantees. *Engineering*, 33:77–89, 2024.

[38] D. Fu, X. Li, L. Wen, M. Dou, P. Cai, B. Shi, and Y. Qiao. Drive like a human: Rethinking autonomous driving with large language models. In *Proceedings of the IEEE/CVF Winter Conference on Applications of Computer Vision*, pages 910–919, 2024.

[39] D. Shah, B. Osiński, S. Levine, et al. Lm-nav: Robotic navigation with large pre-trained models of language, vision, and action. In *Conference on robot learning*, pages 492–504. PMLR, 2023.

[40] Y. Yang, Q. Zhang, C. Li, D. S. Marta, N. Batool, and J. Folkesson. Human-centric autonomous systems with llms for user command reasoning. In *Proceedings of the IEEE/CVF Winter Conference on Applications of Computer Vision*, pages 988–994, 2024.

[41] S. Wang, Z. Yu, X. Jiang, S. Lan, M. Shi, N. Chang, J. Kautz, Y. Li, and J. M. Alvarez. Omnidrive: A holistic llm-agent framework for autonomous driving with 3d perception, reasoning and planning. *arXiv preprint arXiv:2405.01533*, 2024.

[42] J. F. Mullen Jr and D. Manocha. Towards robots that know when they need help: Affordance-based uncertainty for large language model planners. *arXiv preprint arXiv:2403.13198*, 2024.

[43] X. Guan, Y. Liu, H. Lin, Y. Lu, B. He, X. Han, and L. Sun. Mitigating large language model hallucinations via autonomous knowledge graph-based retrofitting. In *Proceedings of the AAAI Conference on Artificial Intelligence*, volume 38, pages 18126–18134, 2024.

[44] S. Schömbs, S. Pareek, J. Goncalves, and W. Johal. Robot-assisted decision-making: Unveiling the role of uncertainty visualisation and embodiment. In *Proceedings of the CHI Conference on Human Factors in Computing Systems*, pages 1–16, 2024.

[45] J. Lee, J. Feng, M. Humt, M. G. Müller, and R. Triebel. Trust your robots! predictive uncertainty estimation of neural networks with sparse gaussian processes. In *Conference on Robot Learning*, pages 1168–1179. PMLR, 2022.

[46] I. Gibbs and E. Candes. Adaptive conformal inference under distribution shift. *Advances in Neural Information Processing Systems*, 34:1660–1672, 2021.

[47] R. Kaur, S. Jha, A. Roy, S. Park, E. Dobriban, O. Sokolsky, and I. Lee. idecode: In-distribution equivariance for conformal out-of-distribution detection. In *Proceedings of the AAAI Conference on Artificial Intelligence*, volume 36, pages 7104–7114, 2022.

[48] C. Tyagi and W. Guo. Multi-label classification under uncertainty: A tree-based conformal prediction approach. In *Conformal and Probabilistic Prediction with Applications*, pages 488–512. PMLR, 2023.

[49] A. Derhacobian, J. Guibas, L. Li, and B. Namboothiry. Adaptive prediction sets with class conditional coverage.

[50] O. J. Dunn. Multiple comparisons among means. *Journal of the American statistical association*, 56(293):52–64, 1961.

[51] L. Mlodzian, Z. Sun, H. Berkemeyer, S. Monka, Z. Wang, S. Dietze, L. Halilaj, and J. Luettin. nuscenes knowledge graph-a comprehensive semantic representation of traffic scenes for trajectory prediction. In *Proceedings of the IEEE/CVF International Conference on Computer Vision*, pages 42–52, 2023.

[52] L. Halilaj, J. Luettin, C. Henson, and S. Monka. Knowledge graphs for automated driving. In *2022 IEEE Fifth International Conference on Artificial Intelligence and Knowledge Engineering (AIKE)*, pages 98–105. IEEE, 2022.

[53] J. P. Queralta, J. Taipalmaa, B. C. Pullinen, V. K. Sarker, T. N. Gia, H. Tenhunen, M. Gabbouj, J. Raitoharju, and T. Westerlund. Collaborative multi-robot search and rescue: Planning, coordination, perception, and active vision. *Ieee Access*, 8:191617–191643, 2020.

[54] F. Yazdani, S. Blumenthal, N. Huebel, A. K. Bozcuoğlu, M. Beetz, and H. Bruyninckx. Query-based integration of heterogeneous knowledge bases for search and rescue tasks. *Robotics and Autonomous Systems*, 117:80–91, 2019.

[55] J. H. Kwak, J. Lee, J. J. Whang, and S. Jo. Semantic grasping via a knowledge graph of robotic manipulation: A graph representation learning approach. *IEEE Robotics and Automation Letters*, 7(4):9397–9404, 2022.

[56] M. Hanheide, M. Göbelbecker, G. S. Horn, A. Pronobis, K. Sjöö, A. Aydemir, P. Jensfelt, C. Gretton, R. Dearden, M. Janicek, et al. Robot task planning and explanation in open and uncertain worlds. *Artificial Intelligence*, 247:119–150, 2017.

[57] M. Hanheide, C. Gretton, R. W. Dearden, N. A. Hawes, J. L. Wyatt, A. Pronobis, A. Aydemir, M. Göbelbecker, and H. Zender. Exploiting probabilistic knowledge under uncertain sensing for efficient robot behaviour. In *Twenty-Second International Joint Conference on Artificial Intelligence*, 2011.

Supplementary Material for the Paper

Conformal Prediction for Semantically-Aware Autonomous Perception in Urban Environments

A Proofs

A.1 Background For Proofs: Cascaded Conformal Prediction

Cascaded conformal prediction (cascaded-CP) [25] is a technique that allows to prune prediction sets sequentially for a *single task*, using a cascade of different non-conformity scores over m steps. Since different statistical tests are applied to the data set, the multiple hypothesis testing (MHT) problem arises, which leads to an increased family-wise error rate (i.e., false positives), making the CP procedure invalid. Cascaded-CP makes use of p-value correction procedures M, such as Simes corrections, to account for MHT problem. Cascaded-CP is formalized in Theorem A.1.

Theorem A.1 (Cascaded-CP [25]) *For any sequence of non-conformity measures* $(S_1, ..., S_m)$*, which yields p-values* $(P_1, ..., P_m)$ *and* $\alpha \in [0, 1]$*, the prediction set* $C^j(X_{test})$ *at step* $j < m$ *is defined as:*

$$C^j(X_{test}) = \{Y \in \mathcal{Y} : \tilde{P}^y_j > \alpha\} \tag{6}$$

where $\tilde{P}^y_j$ *is the corrected p-values using the procedure* M *for candidate* y *at step* j*. Then* $\forall j \in [1, m]$*,* $C^j(X_{test})$ *satisfies Equation 1, and* $C^m(X_{test}) \subseteq C^j(X_{test})$*.*

In this work, we show that Theorem A.1 can be extended to cover multiple tasks in cascade. Furthermore, in our case the tasks are not required to share the same label space. By constructing a knowledge graph facilitating semantic mapping between tasks, our approach accommodates different tasks. Notably, Cascaded-CP can be seen as a sub-case of our work if all tasks are identical.

A.2 Proof of Theorem 3.1

We consider 2 tasks $\mathcal{T}_c$ and $\mathcal{T}_l$ that are performed sequentially. Our goal is to prove that the prediction set C_l^{KRPS} obtained by performing any CP procedure on the set $C_l^{\mathcal{K}}$, which represents the semantic mapping $\mathcal{M}_{c\to l}$ of the set C_c^{KRPS}, satisfies 2 properties: marginal coverage, and semantic consistency with respect to C_c^{KRPS} and $\mathcal{K}$.

Marginal Coverage First, we prove the marginal coverage property of the set C_l^{KRPS}, that is:

$$\mathbb{P}[Y_{test}^l \in C_l^{KRPS}(X_{test})] \geq 1-\alpha \tag{7}$$

The set C_c^{KRPS} is constructed using a CP procedure, meaning that it satisfies Equation 1, and we have:

$$\mathbb{P}[Y_{test}^c \in C_c^{KRPS}(X_{test})] \geq 1-\alpha \tag{8}$$

The semantic mapping $\mathcal{M}_{c\to l}$ is a deterministic mapping that assigns a set of possible locations to each element of $C_c^{KRPS}(X_{test})$. Knowing that the true value of the subsequent task Y_{test}^l is the image of the true value of the starting task Y_{test}^c, the resulting mapping set $C_l^{\mathcal{K}}(X_{test}) = \mathcal{M}_{c\to l}(C_c^{KRPS}(X_{test}))$ contains the Y_{test}^l with a probability that is at least equal to $1-\alpha$, as expressed in Equation 9.

$$\mathbb{P}[Y_{test}^l \in C_l^{\mathcal{K}}(X_{test})] \geq 1-\alpha \tag{9}$$

From the CP coverage Theorem 2.1, we can conclude the existence of a p-value $P_l^{\mathcal{K}}$ that satisfies:

$$\mathbb{P}[Y_{test}^l \in C_l^{\mathcal{K}}(X_{test})] \geq 1-\alpha \iff \mathbb{P}[P_l^{\mathcal{K}} \leq \alpha] \leq \alpha \tag{10}$$

At this step, we have two distinct p-values for the subsequent task $\mathcal{T}_l$, namely $P_l^{\mathcal{K}}$ and P_l. The p-value $P_l^{\mathcal{K}}$ is employed in the construction of the set $C_l^{\mathcal{K}}$, whereas P_l is utilized for forming the set $C^l(X_{test})$, representing the CP-based set for task $\mathcal{T}_l$ independently of the knowledge provided by the prior task $\mathcal{T}_c$, established on C_c^{KRPS}.

Subsequently, we execute a cascaded-CP procedure using Theorem A.1 on the p-values $P_l, P_l^{\mathcal{K}}$. We incorporate a p-value correction procedure denoted as M, resulting in corrected p-values $\tilde{P}_l, \tilde{P}_l^{\mathcal{K}}$, and we have:

$$\begin{aligned} &\mathbb{P}[Y_{test}^l \in C^l(X_{test}) \cap C_l^{\mathcal{K}}(X_{test})] \geq 1-\alpha \\ \iff &\mathbb{P}[Y_{test}^l \in C_l^{KRPS}(X_{test})] \geq 1-\alpha \end{aligned}$$

which is the result stated in Equation 3.

Semantic Consistency Our goal now is to show that the newly constructed prediction set C_l^{KRPS} is semantically consistent with respect to C_c^{KRPS} and $\mathcal{K}$. This result of semantic consistency comes from the fact that for each element Y^l of C_l^{KRPS}, we have $Y^l \in C^l(X_{test}) \cap \mathcal{M}_{c\to l}(C^c(X_{test}))$, meaning that $C_l^{KRPS} \subseteq \mathcal{M}_{c\to l}(C^c(X_{test}))$, which gives the semantic consistency property.

Implications of Theorem 3.1 The direct implication of Theorem 3.1 is that we can further refine the prediction sets generated by any CP procedure given $\mathcal{K}$ and a related task, by removing classes that are not semantically consistent with other tasks, without losing the property of marginal coverage, provided that the p-values are properly corrected. The semantic refinement in KRPS plays an additional role in highlighting corner cases. In urban applications, it is typical to start with a basic knowledge graph and incrementally add new class relationships as data becomes available. This process, however, may encounter corner cases or semantic inconsistencies, like vehicles on sidewalks, not covered by the knowledge graph. KRPS addresses these instances by outputting an empty prediction set when a semantically consistent vehicle position cannot be found. This empty

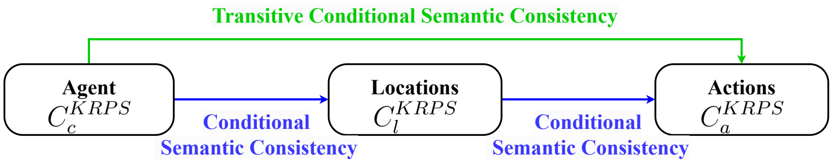

Figure 3: Implications of Theorem 3.1 (blue) and Corollary 3.1 (green) on the semantic consistency.

set signals potential knowledge graph gaps or corner cases, prompting further investigation by end-users. Updating the knowledge graph and performing a calibration step is sufficient to adapt to new data without retraining the model.

A.3 Proof of Corollary 3.1

The sets C_c^{KRPS}, C_l^{KRPS} and, C_a^{KRPS} are 3 prediction sets constructed using KRPS, in the described order. Given this, our goal is to prove that C_a^{KRPS} is semantically consistent with respect to C_c^{KRPS} and $\mathcal{K}$. Since C_a^{KRPS} is constructed based on Theorem 3.1, we have C_a^{KRPS} is semantically consistent with respect to C_l^{KRPS} and $\mathcal{K}$, i.e.,

$$\forall Y_a \in C_a^{KRPS}, \exists Y_l \in C_l^{KRPS} / Y_a \in \mathcal{M}_{l \to a}(Y_l) \tag{11}$$

Since C_l^{KRPS} is constructed using KRPS based on Theorem 3.1, C_l^{KRPS} semantically consistent with respect to C_c^{KRPS} and $\mathcal{K}$ and we have:

$$\forall Y_l \in C_l^{KRPS}, \exists Y_c \in C_c^{KRPS} | Y_l \in \mathcal{M}_{c \to l}(Y_c) \tag{12}$$

Based on Equations 11 and 12, we can establish that:

$$\forall Y_a \in C_a^{KRPS}, \exists Y_c \in C_c^{KRPS} | Y_a \in \mathcal{M}_{c \to a}(Y_c) \tag{13}$$

Which gives that C_a^{KRPS} is semantically consistent with respect to C_c^{KRPS} and $\mathcal{K}$.

Implications of Corollary 3.1 Corollary 3.1 establishes the transitive properties of semantic consistency, as defined using Definition 3.1. As depicted in Figure 3, this result implies that two prediction sets from sequential tasks maintain semantic consistency, even if constructed independently, as long as they are built in sequence relative to a shared task in the middle. This finding holds significance as knowledge bases evolve over time with the inclusion of new tasks. Employing KRPS ensures guarantees of semantic consistency with all prior tasks, by uniquely verifying semantic consistency for the latest executed task.

Comments on the Coverage Guarantees of KRPS. The coverage guarantee, as currently framed in Theorem 3.1, holds in expectation over the calibration sets, reflecting the standard practice in conformal prediction to ensure broad applicability and robustness across various operational scenarios [29]. KRPS prioritizes generalizability and statistical validity across diverse conditions, which is why the guarantee is designed to hold in expectation rather than conditionally. However, KRPS can be easily adapted to conditional coverage guarantees by adopting class conditional calibration procedures, such as in [49].

Comments on the Semantic Consistency Guarantees of KRPS. KRPS guarantees conditional semantic consistency on the prediction sets of the subsequent tasks relative to the first task and the knowledge graph. This means that while KRPS ensures that the sets are semantically consistent given the output of the first task and according to the relationships defined in the knowledge graph, this consistency is conditional on those of initial outputs of the first task executed.

A.4 Details About the Correction Procedure

In our implementation of KRPS, addressing the challenges of multiple hypothesis testing is crucial due to the simultaneous consideration of multiple semantic categories in the knowledge graph. To ensure the validity of our statistical inferences while managing the family-wise error rate (FWER), we employ the Bonferroni correction procedure. The Bonferroni procedure [50] is a conservative approach that adjusts for multiple comparisons by dividing the desired significance level α by the number of hypotheses tested, m.

Specifically, if individual tests are conducted at a significance level α, the Bonferroni correction modifies the significance threshold for each test to $\frac{\alpha}{m}$. For KRPS, where each agent's classification can lead to multiple related hypotheses about actions and locations, the correction ensures that the overall probability of making one or more type I errors does not exceed α.

Mathematically, this is represented as:

$$\alpha_{\text{adjusted}} = \frac{\alpha}{m}$$

Where m is the total number of hypotheses, which corresponds to the number of potential action and location classifications linked to each agent class. By applying the adjustment for the values of α, KRPS maintains the control over the error rates across all tests.

B Structure of the Knowledge Graph

In the following, we provide more details about the knowledge graph used to model the semantic relationships between the entities in the urban environment. We adopt a simple, yet effective ontological model based on the following semantic relationship: *Agent* performs *action* in *location*. It is possible to adopt different task orders, e.g., *Action* is performed in *location* by *agent*. In our setup, the classification of an agent, its location, and its action, correspond to different tasks, that are performed by separate models or separate heads of a single model. This is to ensure that we consider a multitask setup, in contrast to situations where a model outputs a triplet, which we consider as a case of multi-class classification tasks.

We adopt the class labels provided by the ROAD and the Waymo/ROAD++ datasets[5] [1, 24] for all the tasks that we consider. For Completeness, we report the list of agent, location, and action classes, as they are described in the ROAD dataset, in Table 2, Table 3, and Table 4, respectively.

Based on the class labels for each task, the semantic mapping functions $\mathcal{M}_{\mathcal{T}_i \to \mathcal{T}_j}$, where T_i and T_j represent the start and the subsequent tasks, respectively, are constructed through the examination of possible label assignments between the tasks in the training set.

More in details, the construction of the knowledge graph begins by loading semantically coherent triplets from ground truth labels in the training set, which define relationships between agents, actions, and locations. Each agent class is mapped to corresponding action and location classes through boolean arrays within a structured dictionary. The construction procedure ensures also that the reverse mappings can be queried, in case a different sequence task is considered. The knowledge graph construction procedure is detailed in Algorithm 2.

In the KRPS framework, the ground truth data is utilized not merely as examples for training models but also as a fundamental component for constructing the knowledge graph. This dual utilization allows the ground truth data to both train the predictive model and guide the development of semantically aware prediction sets using KRPS, afterwards, ensuring that the prediction sets are statistically valid and semantically consistent across the tasks. Under the assumption of data exchangeability, a central tenet of conformal prediction, we assume that the data in the training, calibration, and test sets come from the same distribution. This assumption helps limit the incompleteness of the knowledge graph construction procedure. Even if the knowledge from the training set is incomplete, KRPS

[5] Waymo/ROAD++: https://sites.google.com/view/road-plus-plus/dataset

manages this by outputting empty sets, prompting the user to address gaps in the knowledge graph or to identify potential anomalies from out-of-distribution samples.

It is important to acknowledge that the construction of knowledge graphs can be approached through various methodologies beyond the one implemented in KRPS. The method described herein was selected for its simplicity and effectiveness within our application scope. Alternative methods, such as [51, 52], demonstrate the capacity to construct complex knowledge graphs tailored to autonomous driving scenarios using different types of input data and for various tasks, such as perception and navigation. Such versatility not only illustrates the scalability of knowledge graph construction processes but also supports their adaptability across different semantic dimensions.

Algorithm 2: Construction of the Knowledge Graph

```
Input  : $GT_{file}$:Ground truth annotations containing agent, action, and location classes from
         training set.
Output: $\mathcal{K}$: A dictionary representing the knowledge graph where agent classes are linked to
         semantically coherent actions and locations.
procedure BuildKnowledgeGraph
    Load ground truth labels from $GT_{file}$
    Extract semantically coherent triplets of agents, actions, and locations
    Initialize an empty dictionary for the knowledge graph
    For each agent class:
        Create a sub-dictionary for actions and locations
        Initialize boolean arrays for actions and locations based on class counts
    Populate the boolean arrays using triplet data:
        For each triplet:
            Mark the corresponding action and location as semantically coherent
    Return the constructed knowledge graph, $\mathcal{K}$
end procedure
```

B.1 Complete Structure of the Knowledge Graph

In the following, we detail the finalized knowledge graph utilized in our implementation. Table 5 summarizes the semantic mappings $\mathcal{M}_{c\to a}$ and $\mathcal{M}_{c\to l}$. The semantic mappings $\mathcal{M}_{a\to c}$ and $\mathcal{M}_{a\to l}$ are represented in Table 6. Finally, the semantic mappings $\mathcal{M}_{l\to c}$ and $\mathcal{M}_{l\to a}$ are represented in Table 7.

B.2 Impact of the Knowledge Graph Size on KRPS

In this section, we systematically evaluate the influence of knowledge graph completeness on the performance of KRPS. Motivated by the necessity to ascertain how the granularity and extent of semantic data affect predictive outcomes, the completeness of the knowledge graph is varied at

Label Name	Abbreviation
Car	Car
Medium Vehicle	MedVeh
Large Vehicle	LarVeh
Bus	Bus
Motorbike	Mobike
Emergency Vehicle	EmVeh
Pedestrian	Ped
Cyclist	Cyc
Vehicle Traffic Light	TL
Other Traffic Light	OthTL

Table 2: List of agent classes and their abbreviations as reported in the ROAD dataset [1].

Label	Abbreviation
In vehicle lane	VehLane
In outgoing lane	OutgoLane
In incoming lane	IncomLane
In outgoing cycle lane	OutgoCycLane
In incoming cycle lane	IncomCycLane
On left pavement	LftPav
On right pavement	RhtPav
On pavement	Pav
At junction	Jun
At crossing	Xing
At bus stop	BusStop
At parking	parking

Table 3: List of used location classes and their abbreviations as reported in the ROAD dataset [1].

Label	Abbreviation
Moving away	MovAway
Moving towards	MovTow
Moving	Mov
Braking	Brake
Stopped	Stop
Indicating left	IncatLft
Indicating right	IncatRht
Hazard lights on	HazLit
Turning left	TurnLft
Turning right	TurnRht
Moving right	MovRht
Moving left	MovLft
Overtaking	Ovtak
Waiting to cross	Wait2X
Crossing road from left	XingFmLft
Crossing road from right	XingFmRht
Crossing	Xing
Pushing object	PushObj
Traffic light red	Red
Traffic light amber	Amber
Traffic light green	Green

Table 4: List of used action classes and their abbreviations as reported in the ROAD dataset [1]

Agent	List of Actions	List of Locations
Ped	MovAway,MovTow,Mov,Stop,Wait2X,XingFmLft,XingFmRht,	VehLane,IncomLane,Pav,LftPav,RhtPav,Jun,xing,BusStop
Car	MovAway,MovTow,Brake,Stop,IncatLft,IncatRht,TurLft,TurRht	VehLane,OutgoLane,IncomLane,Jun
Cyc	MovAway,MovTow,Stop,TurLft,XingFmLft	VehLane,OutgoLane,OutgoCycLane,IncomLane,IncomCycLane
Mobike	MovAway,MovTow,Brake,Stop,IncatLft,IncatRht,TurLft,TurRht	VehLane,OutgoLane,IncomLane,Jun
MedVeh	MovTow,Stop,TurRht, TurLft, Brake	IncomLane,Jun,OutgoLane
LarVeh	MovTow,Stop,TurRht, TurLft, Brake	IncomLane,Jun,OutgoLane
Bus	MovTow,Stop,XingFmLft	VehLane,IncomLane,Jun, BusStop

Table 5: The semantic mappings between the agent classes and the action classes ($\mathcal{M}_{c\to a}$), and the agent classes and the location classes ($\mathcal{M}_{c\to l}$).

Action	List of Agents	List of Locations
MovAway	Ped,Car,Cyc,MedVeh,Bus,LarVeh	VehLane,OutgoLane,OutgoCycLane,Pav,LftPav,RhtPav,Jun
MovTow	Ped,Car,Cyc,MedVeh,Bus,LarVeh	VehLane,IncomLane,IncomCycLane,LftPav,RhtPav,Jun
Mov	Ped	Pav
Brake	Car	VehLane,Jun
Stop	Ped,Car,Cyc,MedVeh,Bus	VehLane,IncomLane,IncomCycLane,Pav,LftPav,RhtPav,Jun,BusStop
IncatLft	Car	VehLane,Jun
IncatRht	Car	IncomLane,Jun
TurLft	Car,Cyc	VehLane,Jun
TurRht	Car,MedVeh	IncomLane,Jun
Ovtak	Car	VehLane
Wait2X	Ped	LftPav,RhtPav
XingFmLft	Ped,Car,Cyc,Bus	VehLane,IncomLane,Jun,xing
XingFmRht	Ped	VehLane,IncomLane,RhtPav,Jun
Xing	Ped,Cyc	Xing
PushObj	Ped	LftPav,RhtPav

Table 6: The semantic mappings between the action classes and the agent classes ($\mathcal{M}_{a \to c}$), and the agent classes and location classes ($\mathcal{M}_{a \to l}$).

Location	List of Agents	List of Actions
VehLane	Ped,Car,Cyc,Bus	MovAway,MovTow,Brake,Stop,IncatLft,TurLft,XingFmLft,XingFmRht
OutgoLane	Car,Cyc	MovAway
OutgoCycLane	Cyc	MovAway
IncomLane	Ped,Car,Cyc,MedVeh,Bus	MovTow,Stop,IncatRht,TurRht,XingFmLft,XingFmRht
IncomCycLane	Cyc	MovTow,Stop
Pav	Ped	MovAway,Mov,Stop
LftPav	Ped,Cyc	MovAway,MovTow,Stop,Wait2X,PushObj
RhtPav	Ped	MovAway,MovTow,Stop,Wait2X,XingFmRht,PushObj
Jun	Ped,Car,Cyc,MedVeh,Bus	MovAway,MovTow,Brake,Stop,IncatLft,IncatRht,TurLft,TurRht,XingFmLft,XingFmRht
xing	Ped	XingFmLft
BusStop	Ped,Bus	Stop
parking	Car	parking

Table 7: The semantic mappings between the location classes and the agent classes ($\mathcal{M}_{l \to c}$), and the location classes and action classes ($\mathcal{M}_{l \to a}$).

50%, 70%, and 90% of its full capacity. The Results in Table 8 report the results on the ROAD dataset with $\alpha = 0.1$ for the $\{agent \to location\}$ sequence, using the "$1 - softmax$" score with KRPS. The results reveal a decrease in semantic consistency corresponding with reduced knowledge graph completeness, although statistical coverage guarantees are maintained. Furthermore the set size is larger with reduced portions of the knowledge graph. This result is expected, as the removed connections from the reduced knowledge graph cannot be used during the refinement process, which impacts the set size and the semantic consistency w.r.t to the full graph. It's important to note that while semantic consistency decreases, Theorem 3.1 and Corollary 3.1 remain valid. This is because these theorems are formulated with respect to the currently used portion of the knowledge graph; therefore, semantic consistency remains perfect (value of 1) when considered within the context of the available graph segment.

Metrics	% of used knowledge graph			
	50%	70%	90%	100%
DTC	0.07	0.06	0.05	**0.02**
SS	6.82	6.53	5.96	**5.86**
SC (w.r.t full K)	0.83	0.86	0.98	**1.00**
SC (w.r.t reduced K)	1.00	1.00	1.00	**1.00**

Table 8: Effects of the knowledge graph size on the performance of KRPS. We evaluate the performance of KRPS with different sizes of the knowledge graph (50%, 70%, 90%) and compare it to the reference of 100% of the knowledge graph (designated in **Bold** in the table). The results are obtained for $\alpha = 0.1$ for the $\{agent \to location\}$ sequence, using the "$1 - softmax$" score with KRPS.

Task	Score	Method	$\alpha = 0.1$			$\alpha = 0.2$			$\alpha = 0.3$			$\alpha = 0.4$			$\alpha = 0.5$		
			SS	DTC	SC	SS	DTC	SC	SS	DTC	SC	SS	DTC	SC	SS	DTC	SC
Location	APS	Stand	7.12	0.05	0.80	6.07	0.10	0.79	5.58	0.16	0.69	4.61	0.20	0.76	4.20	0.27	0.61
		KRPS	**5.90**	**0.02**	**1.00**	**4.96**	**0.05**	**1.00**	**4.05**	**0.01**	**1.00**	**3.65**	**0.12**	**1.00**	**2.61**	**0.00**	**1.00**
	RAPS	Stand	2.66	0.07	0.89	2.03	0.15	0.93	1.70	0.25	0.95	1.56	0.34	0.96	1.46	0.43	0.95
		KRPS	**2.18**	**0.05**	**1.00**	**1.78**	**0.13**	**1.00**	**1.58**	**0.14**	**1.00**	**1.45**	**0.13**	**1.00**	**1.36**	**0.22**	**1.00**
Action	APS	Stand	9.77	0.05	0.75	8.01	0.10	0.73	8.14	0.20	0.72	5.72	0.30	0.70	6.56	0.14	0.69
		KRPS	**7.29**	**0.02**	**1.00**	**6.01**	**0.03**	**1.00**	**5.59**	**0.01**	**1.00**	**4.35**	**0.11**	**1.00**	**3.94**	**0.00**	**1.00**
	RAPS	Stand	4.67	0.07	0.84	3.94	0.13	0.87	3.99	0.23	0.86	2.54	0.25	0.92	2.95	0.37	0.91
		KRPS	**3.82**	**0.03**	**1.00**	**3.26**	**0.02**	**1.00**	**3.27**	**0.13**	**1.00**	**2.22**	**0.15**	**1.00**	**2.52**	**0.17**	**1.00**

Table 9: Results on the ROAD dataset for the task sequences $\{agent \rightarrow location\}$ and $\{agent \rightarrow action\}$.

Task	Score	Method	$\alpha = 0.1$			$\alpha = 0.2$			$\alpha = 0.3$			$\alpha = 0.4$			$\alpha = 0.5$		
			SS	DTC	SC	SS	DTC	SC	SS	DTC	SC	SS	DTC	SC	SS	DTC	SC
Location	APS	Stand	9.02	0.07	0.79	7.92	0.10	0.76	5.97	0.18	0.73	4.03	0.22	0.71	3.98	0.29	0.64
		KRPS	**7.50**	**0.01**	**1.00**	**5.99**	**0.06**	**1.00**	**4.00**	**0.01**	**1.00**	**3.24**	**0.14**	**1.00**	**2.73**	**0.05**	**1.00**
	RAPS	Stand	2.45	0.09	0.87	2.07	0.15	0.91	1.87	0.23	0.93	1.83	0.34	0.96	1.40	0.40	0.95
		KRPS	**2.01**	**0.04**	**1.00**	**2.04**	**0.10**	**1.00**	**1.35**	**0.14**	**1.00**	**1.17**	**0.09**	**1.00**	**1.10**	**0.09**	**1.00**
Action	APS	Stand	10.41	0.05	0.77	6.84	0.13	0.74	6.02	0.15	0.74	5.36	0.12	0.78	4.83	0.20	0.68
		KRPS	**5.98**	**0.02**	**1.00**	**4.18**	**0.02**	**1.00**	**3.90**	**0.07**	**1.00**	**3.87**	**0.12**	**1.00**	**3.94**	**0.08**	**1.00**
	RAPS	Stand	4.36	0.06	0.87	3.03	0.15	0.89	2.48	0.16	0.86	1.50	0.24	0.94	1.20	0.37	0.90
		KRPS	**3.57**	**0.04**	**1.00**	**2.88**	**0.02**	**1.00**	**2.03**	**0.09**	**1.00**	**1.07**	**0.07**	**1.00**	**1.02**	**0.10**	**1.00**

Table 10: Results on the Waymo/ROAD++ dataset for the task sequences $\{agent \rightarrow location\}$ and $\{agent \rightarrow action\}$.

C Results for Further Task Sequences

In Section 4.5, we reported results for sequences of 2 tasks: $\{agent \rightarrow location\}$ and $\{agent \rightarrow action\}$ for $\alpha = [0.1, 0.2, 0.4]$. In the following, we present more results on both datasets for the full set of values of $\alpha = [0.1, 0.2, 0.3, 0.4, 0.5]$ for the sequences $\{agent \rightarrow location\}$ and $\{agent \rightarrow action\}$ in Table 9 and Table 10, respectively. Furthermore, we present results using sequences of 3 tasks on the ROAD dataset to show the capability of KRPS to handle sequences with higher numbers of tasks and in different task orders. The 3-tasks sequences that we consider are: $Seq1 : \{agent \rightarrow action \rightarrow location\}$, and $Seq2 : \{location \rightarrow action \rightarrow agent\}$. We use the same evaluation set-up and data splits reported in the evaluation section in our paper. The results are reported in Table11 and Table 12, respectively.

In all task sequences, KRPS still holds the theoretical coverage guarantees for all values of α. More importantly, KRPS achieves the desired coverage rates while being able to reduce the set size considerably. The conditional semantic consistency also holds, as it is guaranteed by Theorem 3.1 and Corollary 3.1. For all task sequences, the conditional semantic consistency for task 2 with respect to task 1 and $\mathcal{K}$, task 3 with respect to task 2 and $\mathcal{K}$, and task 3 with respect to task 1 and $\mathcal{K}$, is 100%.

D Qualitative Results

In this section, we present further qualitative results on the ROAD and Waymo/ROAD++ datasets for the task sequences $\{agent \rightarrow action\}$, $\{agent \rightarrow location\}$, and $\{agent \rightarrow action \rightarrow location\}$.

Task	Score	Method	$\alpha = 0.1$			$\alpha = 0.2$			$\alpha = 0.3$			$\alpha = 0.4$			$\alpha = 0.5$		
			SS	DTC	SC	SS	DTC	SC	SS	DTC	SC	SS	DTC	SC	SS	DTC	SC
Action	APS	Stand	9.82	0.05	0.71	8.14	0.10	0.65	6.91	0.15	0.61	5.87	0.21	0.58	5.10	0.26	0.56
		KRPS	**7.12**	**0.01**	**1.00**	**5.84**	**0.02**	**1.00**	**4.79**	**0.00**	**1.00**	**3.88**	**0.01**	**1.00**	**3.17**	**0.00**	**1.00**
	RAPS	Stand	4.73	0.07	0.84	3.98	0.13	0.87	3.16	0.18	0.9	2.61	0.26	0.92	2.20	0.33	0.93
		KRPS	**3.84**	**0.06**	**1.00**	**3.26**	**0.12**	**1.00**	**2.65**	**0.17**	**1.00**	**2.24**	**0.15**	**1.00**	**1.93**	**0.21**	**1.00**
Location	APS	Stand	7.67	0.05	0.83	6.77	0.14	0.82	6.19	0.21	0.80	5.80	0.22	0.78	5.31	0.24	0.77
		KRPS	**6.33**	**0.01**	**1.00**	**5.30**	**0.00**	**1.00**	**4.53**	**0.08**	**1.00**	**3.86**	**0.00**	**1.00**	**3.23**	**0.01**	**1.00**
	RAPS	Stand	3.03	0.07	0.90	2.38	0.16	0.94	2.04	0.25	0.95	1.83	0.35	0.96	1.69	0.35	0.96
		KRPS	**2.06**	**0.07**	**1.00**	**2.12**	**0.16**	**1.00**	**1.80**	**0.04**	**1.00**	**1.69**	**0.13**	**1.00**	**1.57**	**0.13**	**1.00**

Table 11: Results on the ROAD dataset for the task sequence $\{agent \rightarrow action \rightarrow location\}$.

Task	Score	Method	$\alpha = 0.1$			$\alpha = 0.2$			$\alpha = 0.3$			$\alpha = 0.4$			$\alpha = 0.5$		
			SS	DTC	SC	SS	DTC	SC	SS	DTC	SC	SS	DTC	SC	SS	DTC	SC
Action	APS	Stand	9.82	0.05	0.72	8.15	0.00	0.68	6.91	0.15	0.64	5.87	0.21	0.60	5.10	0.26	0.58
		KRPS	**7.35**	**0.00**	**1.00**	**6.02**	**0.00**	**1.00**	**4.91**	**0.00**	**1.00**	**3.97**	**0.00**	**1.00**	**3.20**	**0.01**	**1.00**
	RAPS	Stand	4.73	0.07	0.82	3.98	0.15	0.85	3.16	0.20	0.89	2.61	0.26	0.91	2.20	0.35	0.92
		KRPS	**3.86**	**0.06**	**1.00**	**3.24**	**0.13**	**1.00**	**2.64**	**0.18**	**1.00**	**2.23**	**0.25**	**1.00**	**1.93**	**0.32**	**1.00**
Agent	APS	Stand	7.00	0.06	0.53	6.52	0.13	0.54	6.16	0.20	0.55	5.76	0.27	0.56	5.48	0.33	0.55
		KRPS	**3.45**	**0.00**	**1.00**	**3.07**	**0.00**	**1.00**	**2.74**	**0.00**	**1.00**	**2.36**	**0.00**	**1.00**	**2.03**	**0.01**	**1.00**
	RAPS	Stand	1.55	0.08	0.92	1.31	**0.08**	0.92	1.22	0.27	0.97	1.16	0.27	0.97	1.13	0.26	0.95
		KRPS	**1.31**	**0.08**	**1.00**	**1.19**	0.10	**1.00**	**1.14**	**0.17**	**1.00**	**1.11**	**0.27**	**1.00**	**1.08**	**0.26**	**1.00**

Table 12: Results on the ROAD dataset for the task sequence $\{location \rightarrow action \rightarrow agent\}$.

D.1 Qualitative Results on the ROAD Dataset

Figure 4 shows 3 different scenes from the ROAD dataset with the agent of interest highlighted with the red bounding box. For each bounding box, we perform the indicated CP procedure to acquire the prediction sets for the agent classification task. Based on the agent prediction sets, we report the generated prediction sets with and without KRPS using the Softmax, APS, and RAPS scores.

Figure 6a shows a scene with a *car stopping in the outgoing lane*. The prediction sets for the action and location classification tasks demonstrate how KRPS achieved a substantial reduction for the prediction sets. This reduction is particularly observable for the location task with the softmax and APS scores, where the prediction set size is reduced by 4 classes.

Figure 4b shows a scene with a *bus stopping in the vehicle lane*. All approaches succeed in including the correct labels in the prediction sets. The combination of KRPS with RAPS succeeds in constructing a singleton for the tasks location and action classification. By applying KRPS, the action and location classes that are not relevant to the agent class are removed.

Figure 6b showcases a scene with a *bus moving towards in the incoming lane*. Using KRPS, the size of the prediction sets for the action classification is reduced by 50% for the softmax score, by 75% for APS, and by 66% for RAPS. For the location classification task, KRPS reduced the prediction set size by 50% for the softmax score, by 50% for APS. For RAPS, the prediction set is not reduced, since both locations, *incoming lane* and *junction* are possible, given the agent class and its action.

The figures highlight the capability of KRPS to reduce the set size by removing action and location classes that are not relevant to the agent. Theorem 3.1 ensures that this removal procedure does not affect the marginal coverage property.

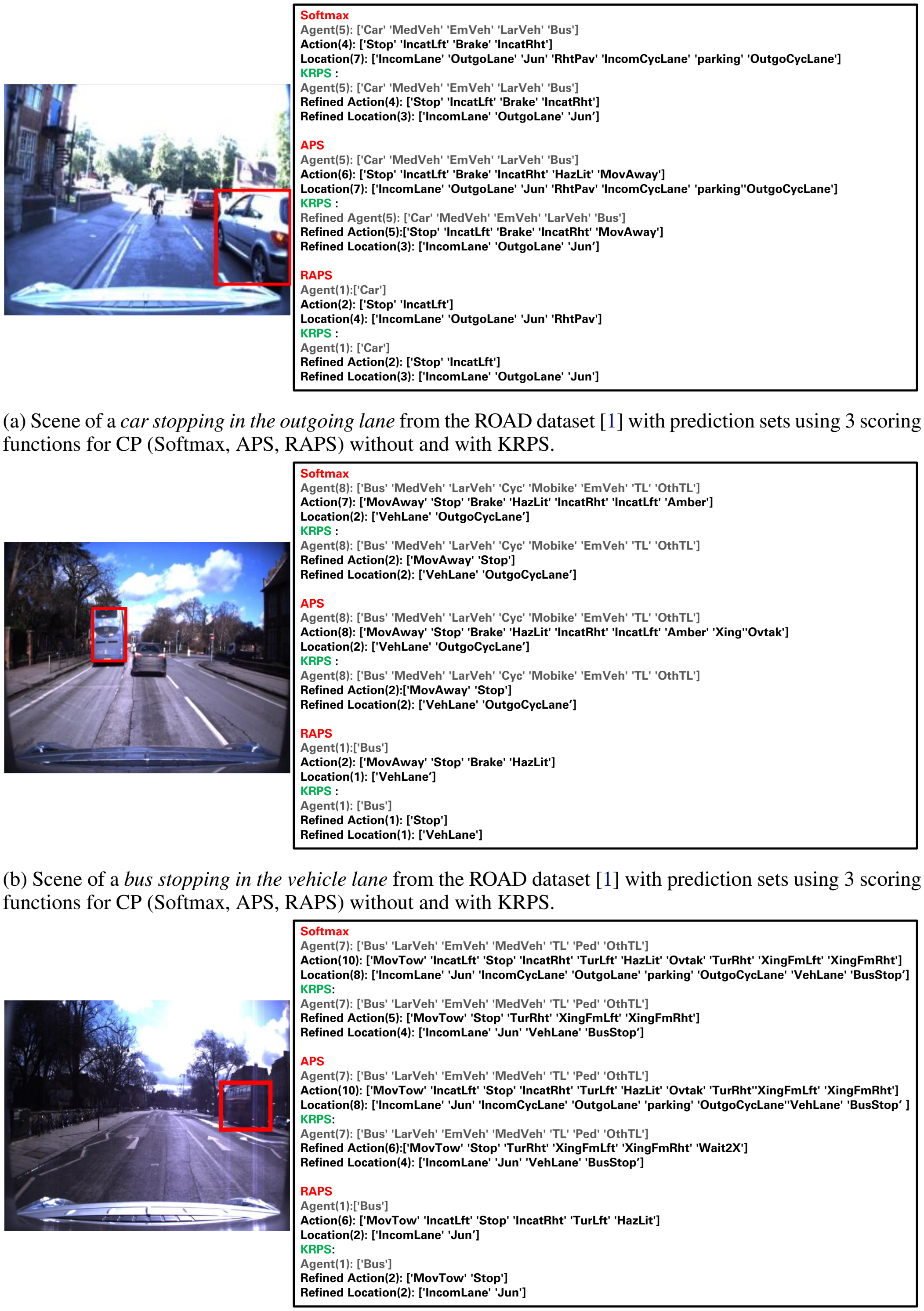

```
Softmax
Agent(5): ['Car' 'MedVeh' 'EmVeh' 'LarVeh' 'Bus']
Action(4): ['Stop' 'IncatLft' 'Brake' 'IncatRht']
Location(7): ['IncomLane' 'OutgoLane' 'Jun' 'RhtPav' 'IncomCycLane' 'parking' 'OutgoCycLane']
KRPS :
Agent(5): ['Car' 'MedVeh' 'EmVeh' 'LarVeh' 'Bus']
Refined Action(4): ['Stop' 'IncatLft' 'Brake' 'IncatRht']
Refined Location(3): ['IncomLane' 'OutgoLane' 'Jun’]

APS
Agent(5): ['Car' 'MedVeh' 'EmVeh' 'LarVeh' 'Bus']
Action(6): ['Stop' 'IncatLft' 'Brake' 'IncatRht' 'HazLit' 'MovAway']
Location(7): ['IncomLane' 'OutgoLane' 'Jun' 'RhtPav' 'IncomCycLane' 'parking''OutgoCycLane']
KRPS :
Refined Agent(5): ['Car' 'MedVeh' 'EmVeh' 'LarVeh' 'Bus']
Refined Action(5):['Stop' 'IncatLft' 'Brake' 'IncatRht' 'MovAway']
Refined Location(3): ['IncomLane' 'OutgoLane' 'Jun’]

RAPS
Agent(1):['Car']
Action(2): ['Stop' 'IncatLft']
Location(4): ['IncomLane' 'OutgoLane' 'Jun' 'RhtPav']
KRPS :
Agent(1): ['Car']
Refined Action(2): ['Stop' 'IncatLft']
Refined Location(3): ['IncomLane' 'OutgoLane' 'Jun']
```

(a) Scene of a *car stopping in the outgoing lane* from the ROAD dataset [1] with prediction sets using 3 scoring functions for CP (Softmax, APS, RAPS) without and with KRPS.

```
Softmax
Agent(8): ['Bus' 'MedVeh' 'LarVeh' 'Cyc' 'Mobike' 'EmVeh' 'TL' 'OthTL']
Action(7): ['MovAway' 'Stop' 'Brake' 'HazLit' 'IncatRht' 'IncatLft' 'Amber']
Location(2): ['VehLane' 'OutgoCycLane’]
KRPS :
Agent(8): ['Bus' 'MedVeh' 'LarVeh' 'Cyc' 'Mobike' 'EmVeh' 'TL' 'OthTL']
Refined Action(2): ['MovAway' 'Stop']
Refined Location(2): ['VehLane' 'OutgoCycLane’]

APS
Agent(8): ['Bus' 'MedVeh' 'LarVeh' 'Cyc' 'Mobike' 'EmVeh' 'TL' 'OthTL']
Action(8): ['MovAway' 'Stop' 'Brake' 'HazLit' 'IncatRht' 'IncatLft' 'Amber' 'Xing''Ovtak']
Location(2): ['VehLane' 'OutgoCycLane’]
KRPS :
Agent(8): ['Bus' 'MedVeh' 'LarVeh' 'Cyc' 'Mobike' 'EmVeh' 'TL' 'OthTL']
Refined Action(2):['MovAway' 'Stop']
Refined Location(2): ['VehLane' 'OutgoCycLane’]

RAPS
Agent(1):['Bus']
Action(2): ['MovAway' 'Stop' 'Brake' 'HazLit']
Location(1): ['VehLane’]
KRPS :
Agent(1): ['Bus']
Refined Action(1): ['Stop']
Refined Location(1): ['VehLane']
```

(b) Scene of a *bus stopping in the vehicle lane* from the ROAD dataset [1] with prediction sets using 3 scoring functions for CP (Softmax, APS, RAPS) without and with KRPS.

```
Softmax
Agent(7): ['Bus' 'LarVeh' 'EmVeh' 'MedVeh' 'TL' 'Ped' 'OthTL']
Action(10): ['MovTow' 'IncatLft' 'Stop' 'IncatRht' 'TurLft' 'HazLit' 'Ovtak' 'TurRht' 'XingFmLft' 'XingFmRht']
Location(8): ['IncomLane' 'Jun' 'IncomCycLane' 'OutgoLane' 'parking' 'OutgoCycLane' 'VehLane' 'BusStop’]
KRPS:
Agent(7): ['Bus' 'LarVeh' 'EmVeh' 'MedVeh' 'TL' 'Ped' 'OthTL']
Refined Action(5): ['MovTow' 'Stop' 'TurRht' 'XingFmLft' 'XingFmRht']
Refined Location(4): ['IncomLane' 'Jun' 'VehLane' 'BusStop’]

APS
Agent(7): ['Bus' 'LarVeh' 'EmVeh' 'MedVeh' 'TL' 'Ped' 'OthTL']
Action(10): ['MovTow' 'IncatLft' 'Stop' 'IncatRht' 'TurLft' 'HazLit' 'Ovtak' 'TurRht''XingFmLft' 'XingFmRht']
Location(8): ['IncomLane' 'Jun' 'IncomCycLane' 'OutgoLane' 'parking' 'OutgoCycLane''VehLane' 'BusStop’ ]
KRPS:
Agent(7): ['Bus' 'LarVeh' 'EmVeh' 'MedVeh' 'TL' 'Ped' 'OthTL']
Refined Action(6):['MovTow' 'Stop' 'TurRht' 'XingFmLft' 'XingFmRht' 'Wait2X']
Refined Location(4): ['IncomLane' 'Jun' 'VehLane' 'BusStop’]

RAPS
Agent(1):['Bus']
Action(6): ['MovTow' 'IncatLft' 'Stop' 'IncatRht' 'TurLft' 'HazLit']
Location(2): ['IncomLane' 'Jun’]
KRPS:
Agent(1): ['Bus']
Refined Action(2): ['MovTow' 'Stop']
Refined Location(2): ['IncomLane' 'Jun']
```

(c) Scene of a *bus moving towards in the incoming lane* from the ROAD dataset [1] with prediction sets using 3 scoring functions for CP (Softmax, APS, RAPS) without and with KRPS.

Figure 4: Scenes from the ROAD dataset [1] with prediction sets using 3 scoring functions for CP (Softmax, APS, RAPS) without and with KRPS.

D.2 Qualitative Results on the Waymo/ROAD++ Dataset

Figure 5 shows 2 different scenes from the Waymo/ROAD++ dataset, characterized by challenging situational and environmental conditions that may induce high uncertainty. The agent of interest is highlighted with the red bounding box. We perform the indicated CP procedure for each bounding box to acquire the prediction sets for the agent classification task. Based on the agent prediction sets, we report the generated prediction sets with and without KRPS using the Softmax, APS, and RAPS scores.

Figure 5a depicts a low-light scenario where a pedestrian crosses the street with a car in the background of the bounding box. The challenging lighting conditions and complex scene composition contribute to uncertainty, prompting the model to assign vehicle-associated actions and locations such as *Brake* and *outgoing lane*. using KRPS mitigates this confusion by restricting the subsequent tasks to consider only classes suitable for pedestrians or bicycles, as determined by the agent classification model. KRPS notably reduces uncertainty and shrinks the prediction set size by 80%, 83%, and 50% for softmax, APS, and RAPS predictions, respectively, for the action classification task. For location classification, the prediction set size is reduced by 50%, 75%, and 50% for softmax, APS, and RAPS, respectively.

Figure 5b illustrates a scenario where a pedestrian is crossing the street while pushing a bicycle. This presence of the bicycle often misleads models for action and location to assign characteristics typical of bicyclists, such as *Brake* and *outgoing lane*. KRPS addresses this issue by ensuring that only classes suitable for either pedestrians or bicycles are considered, as dictated by the initial agent classification results. This application of KRPS significantly reduces uncertainty and narrows the prediction set size by 71%, 60%, and 66% for the softmax, APS, and RAPS predictions for the action classification task, respectively. Similarly, for the location classification task, the prediction set sizes are reduced by 66%, 50%, and 66% for softmax, APS, and RAPS, respectively.

E Further Details About Empty Prediction Sets

In the KRPS framework, the occurrence of empty prediction sets is a critical aspect, designed to signal either anomalies in the detection or significant mismatches and gaps within the knowledge graph. The empty sets arise when no available classes meet the semantic and statistical criteria established by the knowledge graph and conformal prediction rules. In traditional conformal prediction, an empty prediction set is generated when the non-conformity score for any potential prediction exceeds the calibrated threshold, indicating that none of the possible outcomes is statistically plausible within the given confidence level. KRPS enhances the traditional conformal prediction model by integrating a semantic layer that evaluates the coherence of potential predictions with the knowledge graph. This integration means that even if a prediction is statistically plausible, it might still be rejected if it fails to align semantically with the knowledge graph. Hence, empty prediction sets may also occur due to the absence of semantically consistent labels, particularly in scenarios where the knowledge graph does not fully cover all possible real-world variations.

We conduct an experiment to quantify the frequency of empty prediction sets produced by KRPS and compare these outcomes to traditional conformal prediction baselines, to assess the impact of semantic layer in KRPS on the generation of empty sets. The results, depicted in Figure 6, show a trend where $1 - Softmax$, APS, and their combination with KRPS produce more empty sets as the value of α increases, a behavior expected as higher α values lead conformal prediction approaches to generate smaller prediction sets, as they tolerate more risk. This is however different for RAPS, where the percentage of empty sets is zero across the different values of α. This is an expected behavior since the regularization term in RAPS encourages the inclusion of additional labels if the set is too small, thus preventing it from being empty. By adaptively adjusting the threshold for inclusion based on the desired coverage level, RAPS ensures that there is always at least one label that meets the criteria, thereby avoiding empty prediction sets. KRPS, in contrast to the baselines, consistently shows a higher frequency of empty sets due to the semantic consistency checks integrated. If a po-

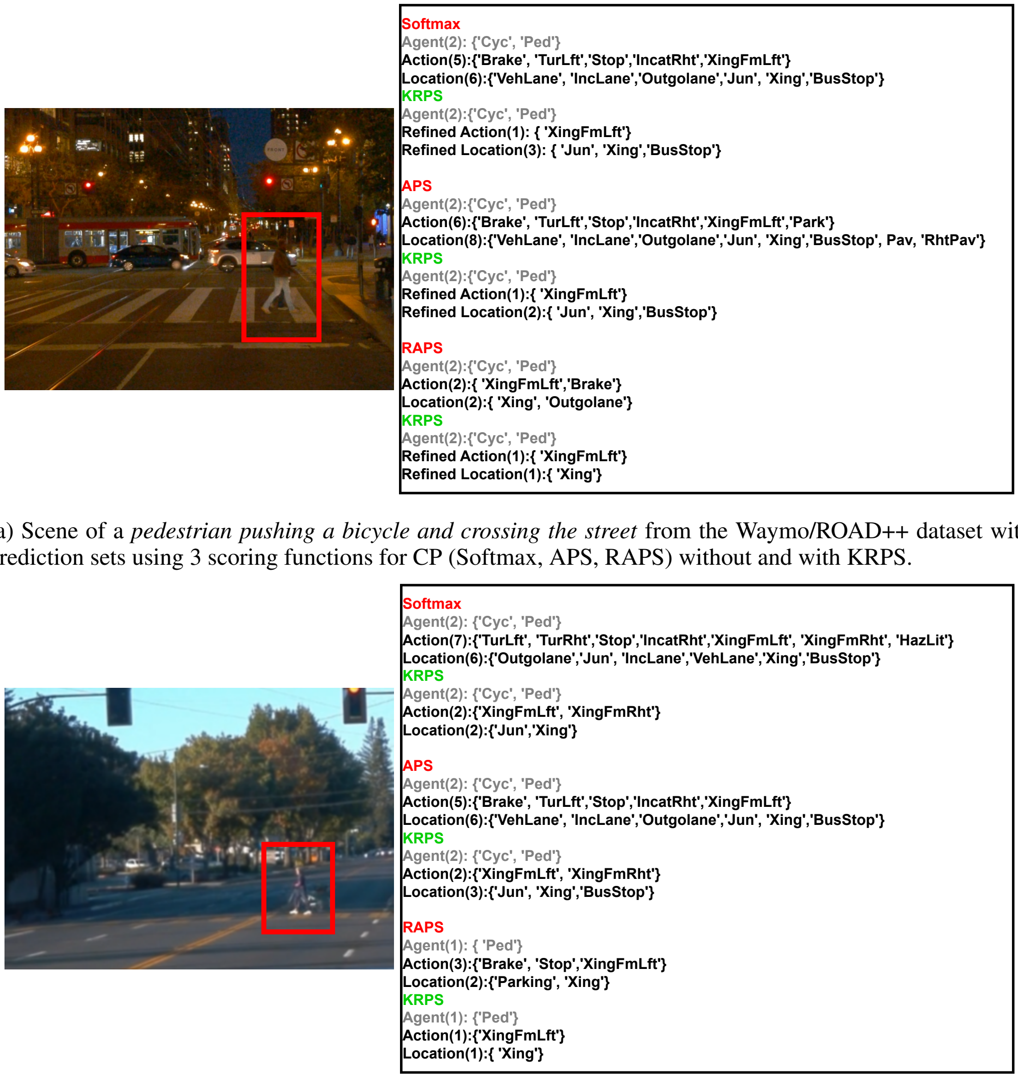

```
Softmax
Agent(2): {'Cyc', 'Ped'}
Action(5):{'Brake', 'TurLft','Stop','IncatRht','XingFmLft'}
Location(6):{'VehLane', 'IncLane','Outgolane','Jun', 'Xing','BusStop'}
KRPS
Agent(2):{'Cyc', 'Ped'}
Refined Action(1): { 'XingFmLft'}
Refined Location(3): { 'Jun', 'Xing','BusStop'}

APS
Agent(2):{'Cyc', 'Ped'}
Action(6):{'Brake', 'TurLft','Stop','IncatRht','XingFmLft','Park'}
Location(8):{'VehLane', 'IncLane','Outgolane','Jun', 'Xing','BusStop', Pav, 'RhtPav'}
KRPS
Agent(2):{'Cyc', 'Ped'}
Refined Action(1):{ 'XingFmLft'}
Refined Location(2):{ 'Jun', 'Xing','BusStop'}

RAPS
Agent(2):{'Cyc', 'Ped'}
Action(2):{ 'XingFmLft','Brake'}
Location(2):{ 'Xing', 'Outgolane'}
KRPS
Agent(2):{'Cyc', 'Ped'}
Refined Action(1):{ 'XingFmLft'}
Refined Location(1):{ 'Xing'}
```

(a) Scene of a *pedestrian pushing a bicycle and crossing the street* from the Waymo/ROAD++ dataset with prediction sets using 3 scoring functions for CP (Softmax, APS, RAPS) without and with KRPS.

```
Softmax
Agent(2): {'Cyc', 'Ped'}
Action(7):{'TurLft', 'TurRht','Stop','IncatRht','XingFmLft', 'XingFmRht', 'HazLit'}
Location(6):{'Outgolane','Jun', 'IncLane','VehLane','Xing','BusStop'}
KRPS
Agent(2): {'Cyc', 'Ped'}
Action(2):{'XingFmLft', 'XingFmRht'}
Location(2):{'Jun','Xing'}

APS
Agent(2): {'Cyc', 'Ped'}
Action(5):{'Brake', 'TurLft','Stop','IncatRht','XingFmLft'}
Location(6):{'VehLane', 'IncLane','Outgolane','Jun', 'Xing','BusStop'}
KRPS
Agent(2): {'Cyc', 'Ped'}
Action(2):{'XingFmLft', 'XingFmRht'}
Location(3):{'Jun', 'Xing','BusStop'}

RAPS
Agent(1): { 'Ped'}
Action(3):{'Brake', 'Stop','XingFmLft'}
Location(2):{'Parking', 'Xing'}
KRPS
Agent(1): {'Ped'}
Action(1):{'XingFmLft'}
Location(1):{ 'Xing'}
```

(b) Scene of a *pedestrian pushing a bicycle and crossing the street* from the Waymo/ROAD++ dataset with prediction sets using 3 scoring functions for CP (Softmax, APS, RAPS) without and with KRPS.

Figure 5: Scenes from the Waymo/ROAD++ dataset with prediction sets using 3 scoring functions for CP (Softmax, APS, RAPS) without and with KRPS.

tential prediction fails to meet both semantic and statistical criteria, KRPS opts to return an empty set, avoiding inaccurate or contextually inappropriate predictions. Conversely, traditional conformal prediction methods, which lack a semantic filter, tend to produce fewer empty sets but at the risk of including predictions that, although statistically plausible, might not align semantically with the context of the scene.

In Figure 7, we show a qualitative example of a situation where KRPS outputs an empty set, while the RAPS does not. The scenario illustrates a car for which the ground truth location is *VehLane*, which indicates a *Vehicle lane*. Applying RAPS using $\alpha = 0.5$ leads to a prediction set including a single class, which is *OutgoCycLane*, referring to an *Outgoing Cycle Lane*. In contrast, when refining the prediction set with KRPS in accordance with the agent class *Car* and the knowledge graph, KRPS yields an empty set. This outcome signals that none of the predicted locations are applicable to the *Car* agent class, prompting considerations of potential anomalies, such as a car mistakenly detected in a cycle lane. It is important to note that had such scenarios been present

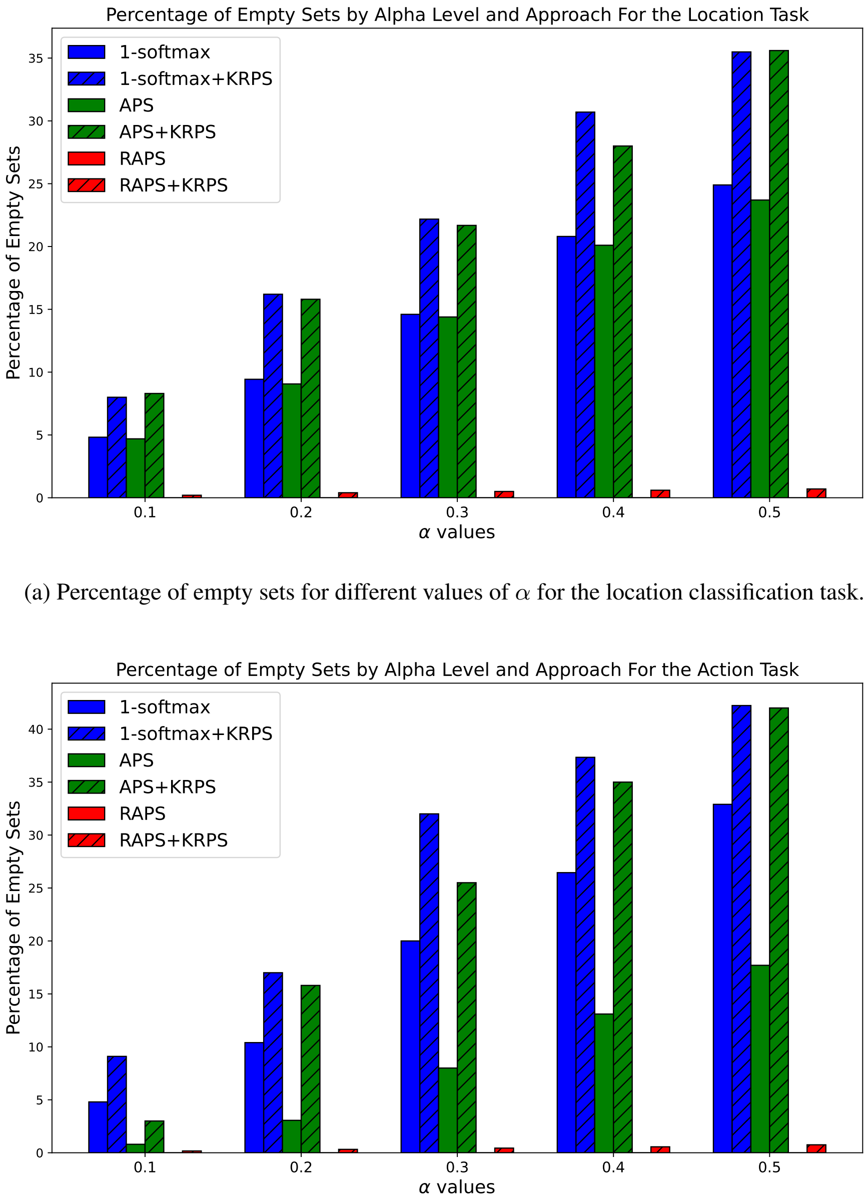

(a) Percentage of empty sets for different values of α for the location classification task.

(b) Percentage of empty sets for different values of α for the action classification task.

Figure 6: Percentage of empty sets for different values of α for the location and action classification tasks based w.r.t the knowledge graph and predictions of the agent class.

in the training data, the knowledge graph would have accounted for them, preventing KRPS from producing an empty set under these conditions.

F More on the Practicality of KRPS

While our paper focuses on three high-level perception tasks for urban scene understanding, KRPS can be extended to other robot perception applications with varying natures and a number of tasks. The formulation of Algorithm 1 and Theorem 3.1 is adaptable to diverse environmental contexts.

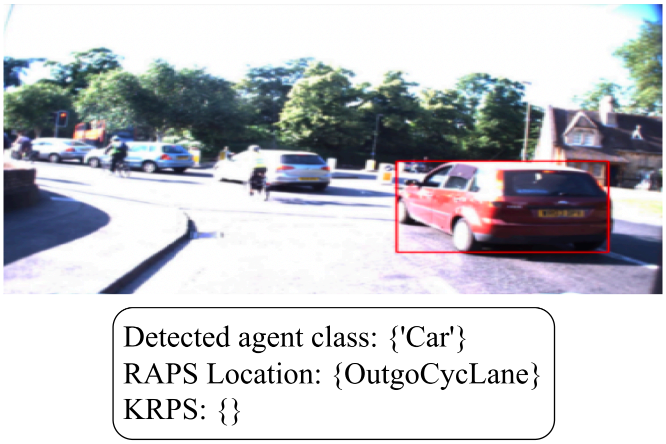

Detected agent class: {'Car'}
RAPS Location: {OutgoCycLane}
KRPS: {}

Figure 7: Qualitative example of empty set generated by KRPS, using RAPS and $\alpha = 0.5$.

For example, KRPS can be applied to urban search and rescue, where tasks such as victim detection, hazard identification, and robot action selection are critical [53]. In this scenario, the detection of victims informs subsequent hazard identification tasks by highlighting areas where hazards are likely to be present. The results from hazard identification can then guide the action selection of the robot, such as navigating safely through debris or delivering emergency supplies. The role of external knowledge in the form of knowledge graphs or other forms of semantics can be decisive for the mission success [54]. KRPS enhances this application by ensuring that each prediction set is semantically consistent with the preceding tasks and by providing uncertainty quantification, which is crucial for making reliable decisions in high-stakes environments.

In the domain of robot manipulation, KRPS can significantly improve the accuracy and reliability of tasks such as object recognition, grasp strategy selection, and precise placement. Here, the classification of objects directly influences the choice of the manipulation action [55]. For instance, identifying an object as fragile necessitates a more delicate grasping approach compared to a robust item. Uncertainty quantification is particularly important in this context to avoid mistakes such as misidentifying an object, which could lead to improper handling and potential damage. KRPS ensures that each stage of the manipulation process is informed by the previous task's outcomes, enhancing both semantic consistency and decision reliability.

Additionally, KRPS can be utilized in robotic navigation, especially in dynamic and unpredictable urban environments. The class of the robot's behavior, such as stopping, turning, or accelerating, can depend on the classes of agents present in the environment and their predicted future maneuvers [56, 57]. For example, the presence of a pedestrian crossing the road might necessitate the robot to stop, while an approaching vehicle could require the robot to yield or change lanes [51, 52]. In this application, KRPS provides a structured way to integrate these interdependent tasks, ensuring that navigation decisions are not only statistically valid but also semantically coherent with the surrounding context. This integration of uncertainty quantification and semantic consistency enables robots to navigate more safely and efficiently, adapting to complex real-world scenarios with greater reliability.